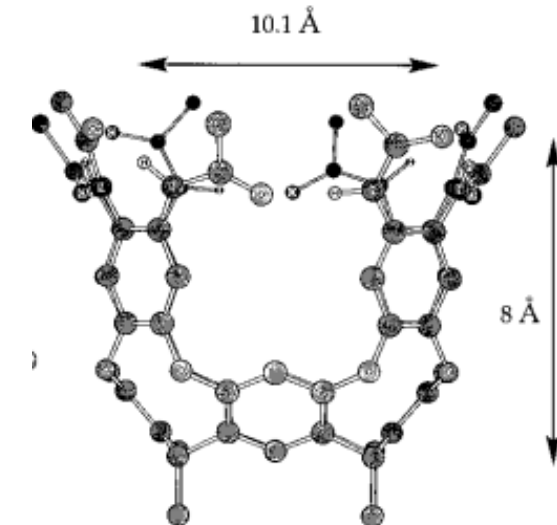
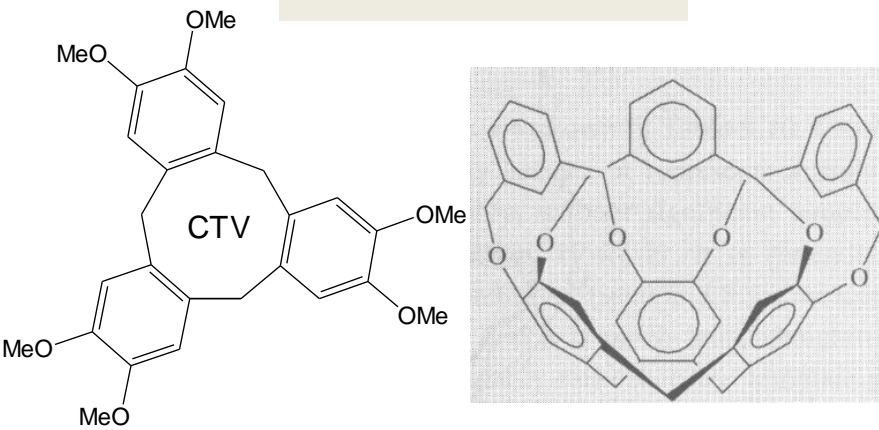
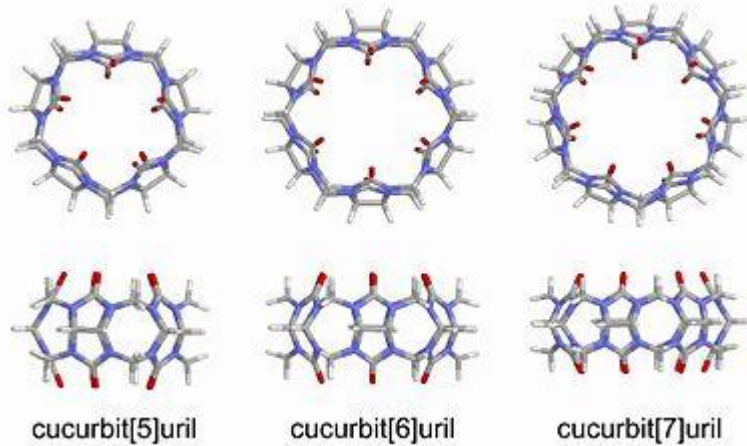


Cavitandi

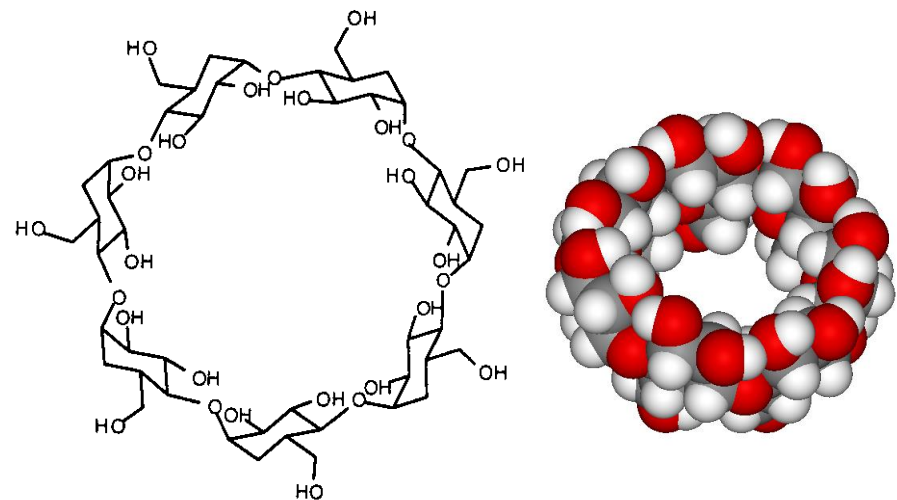
cyclotriferratilene



Cucurbiturili



Ciclodestrine



Capsule Molecolari

Unione di due cavitandi

Connessione covalente

Legame idrogeno

Legame di coordinazione

Pre-organizzazione

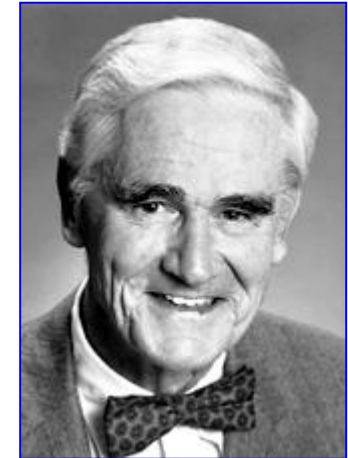
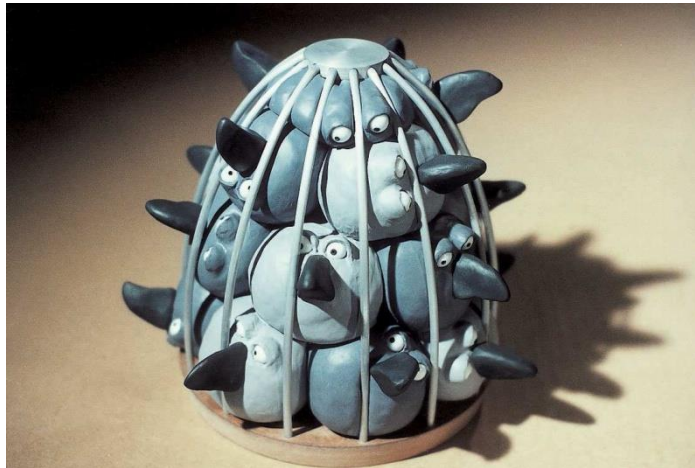
Protezione dal solvente esterno

Rallentamento delle cinetiche di scambio

Stabilizzazione di specie reattive

Reazioni catalitiche

Drug delivery

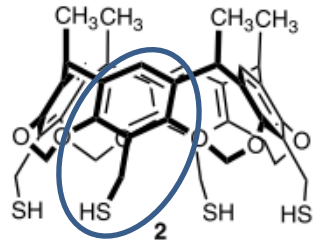


Carcerando:

Contenitore molecolare chiuso (capsula) che definisce cavità sferica, i guest sono intrappolati (all'atto della sintesi) entrata e uscita solo per rottura di legame covalente, i.e. velocità di scambio virtualmente nulla

Carcerandi

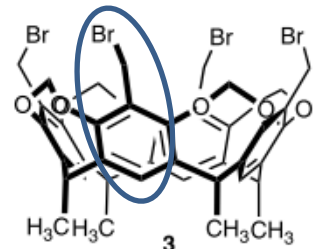
Benzil-tiolo



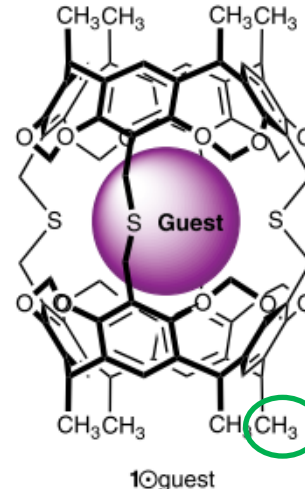
Cs_2CO_3
 $(\text{CH}_3)_2\text{NCHO}$
 $(\text{CH}_2)_4\text{O}$
Ar

29% yield

benzil cloruro
(o bromuro)



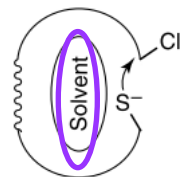
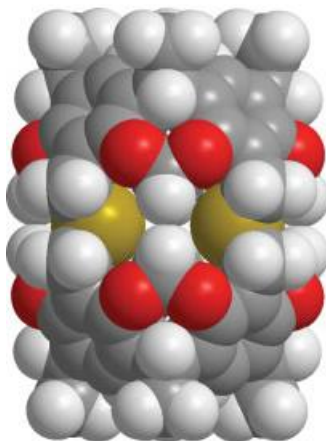
Alta dliuz



Guest: $\text{Cs}^+(\text{CH}_3)_2\text{NCHO}$;
 $(\text{CH}_2)_4\text{O}$; Ar

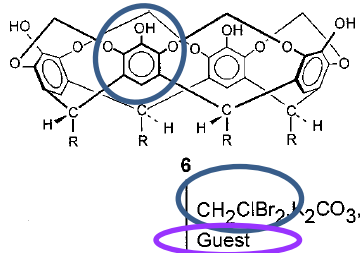
1@Guest

Insolubilità = caratterizz via IR, FAB-MS, analisi elementare, test chimici
FAB-MS dei carcinoplessi

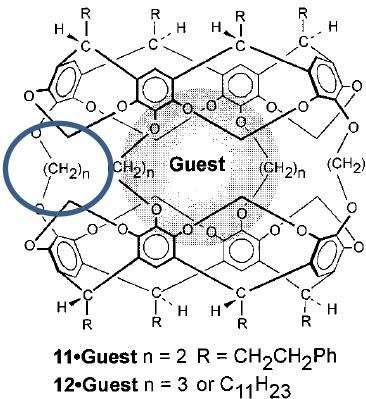
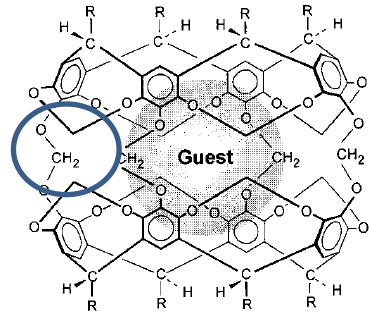


Carcerandi

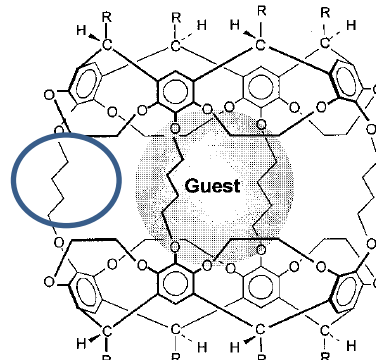
fenolo

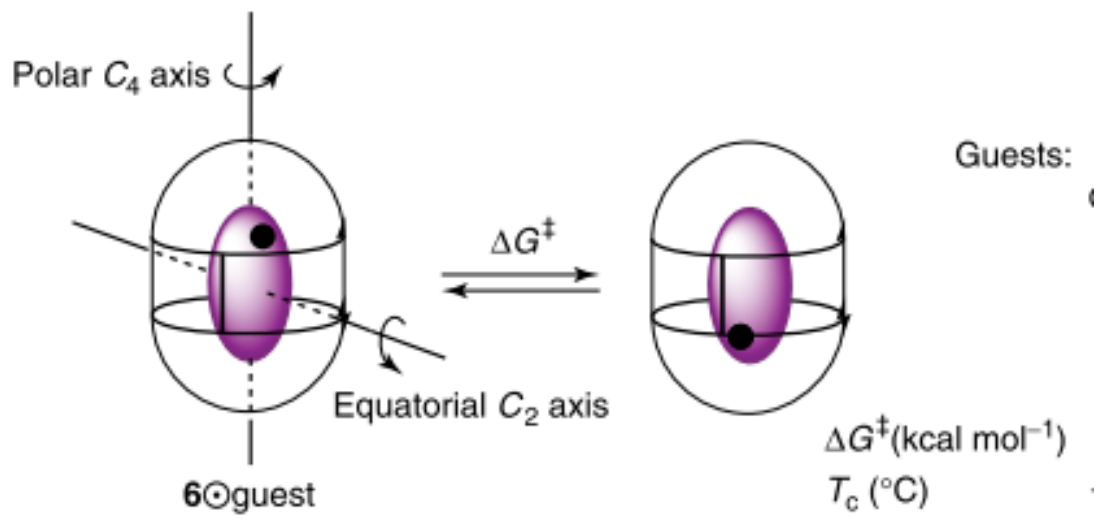


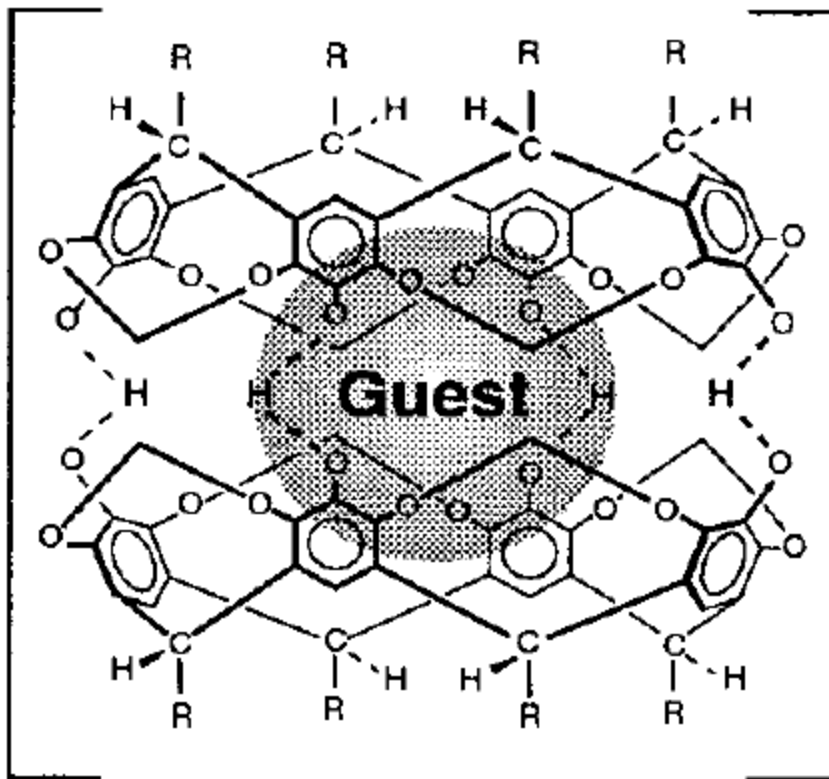
bromo-clorometano



12-Guest n = 3 or C₁₁H₂₃

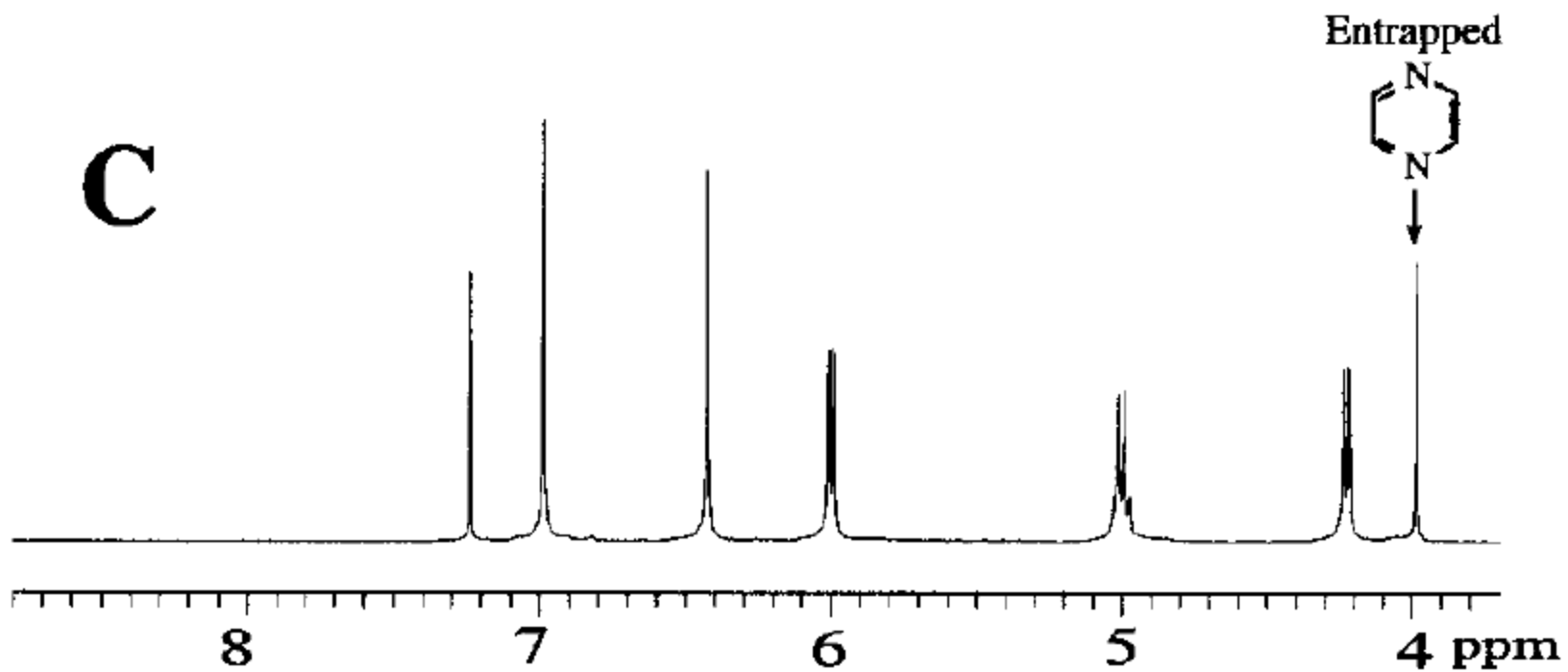


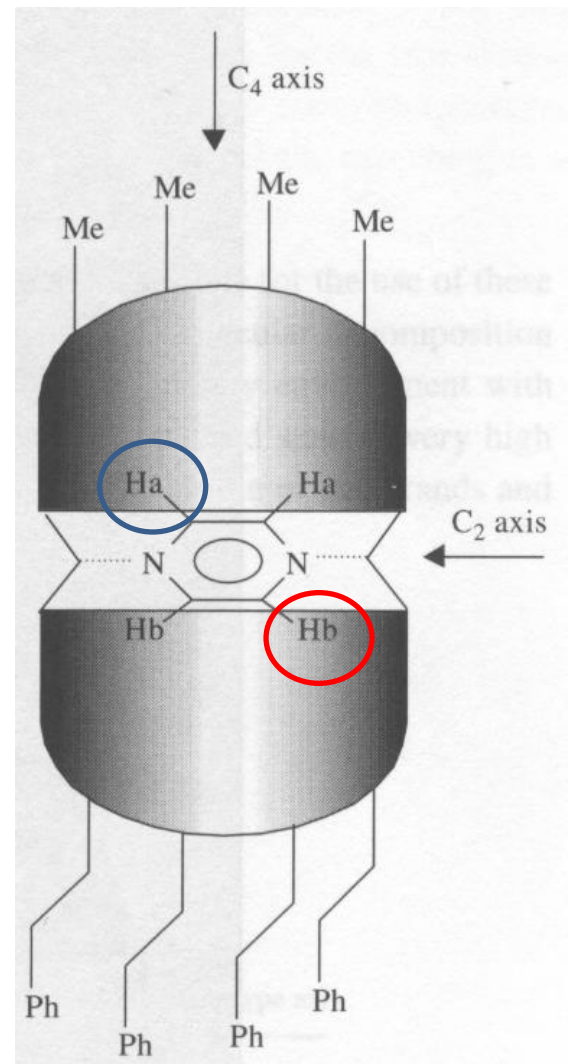


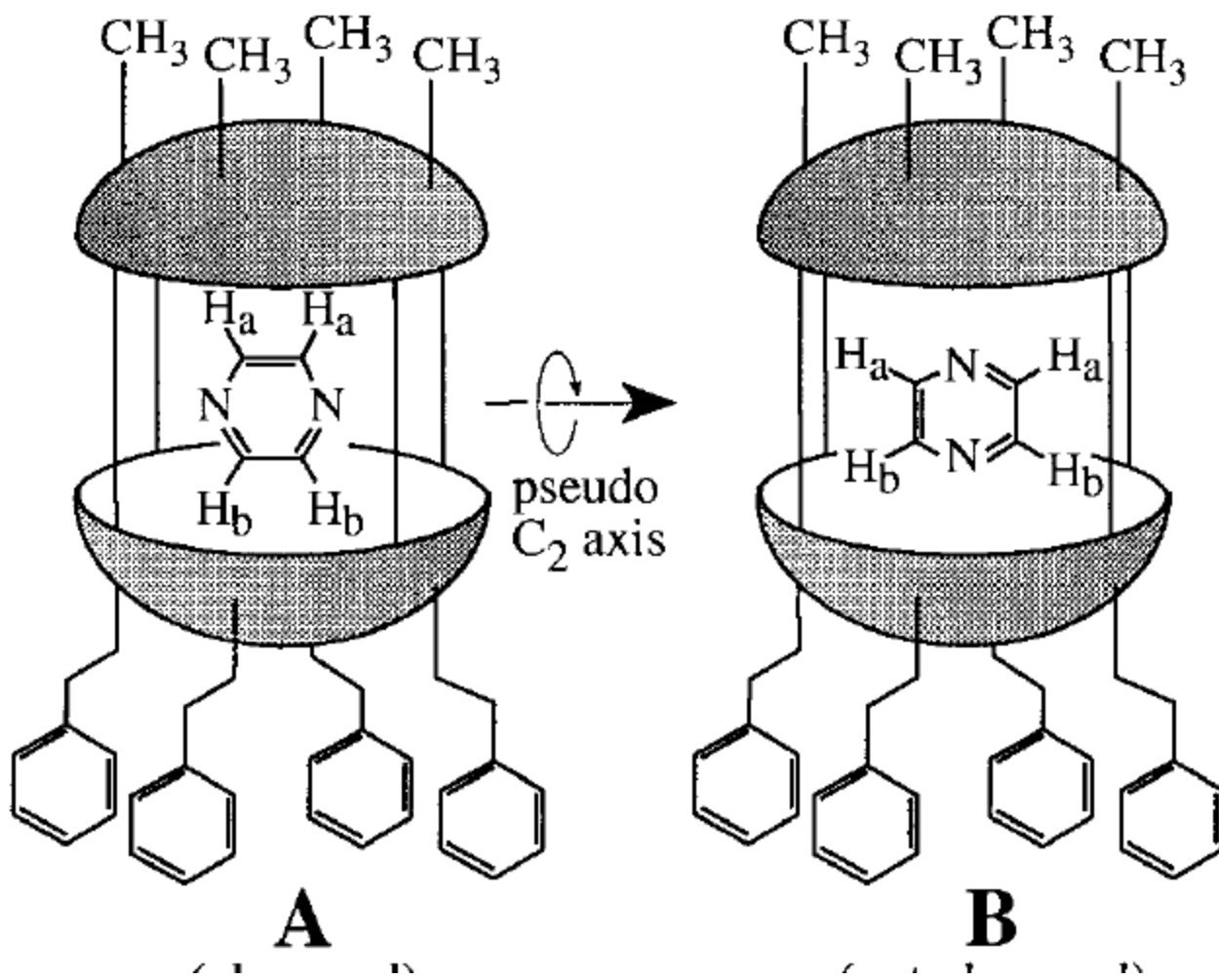


Complex 3•Guest

C

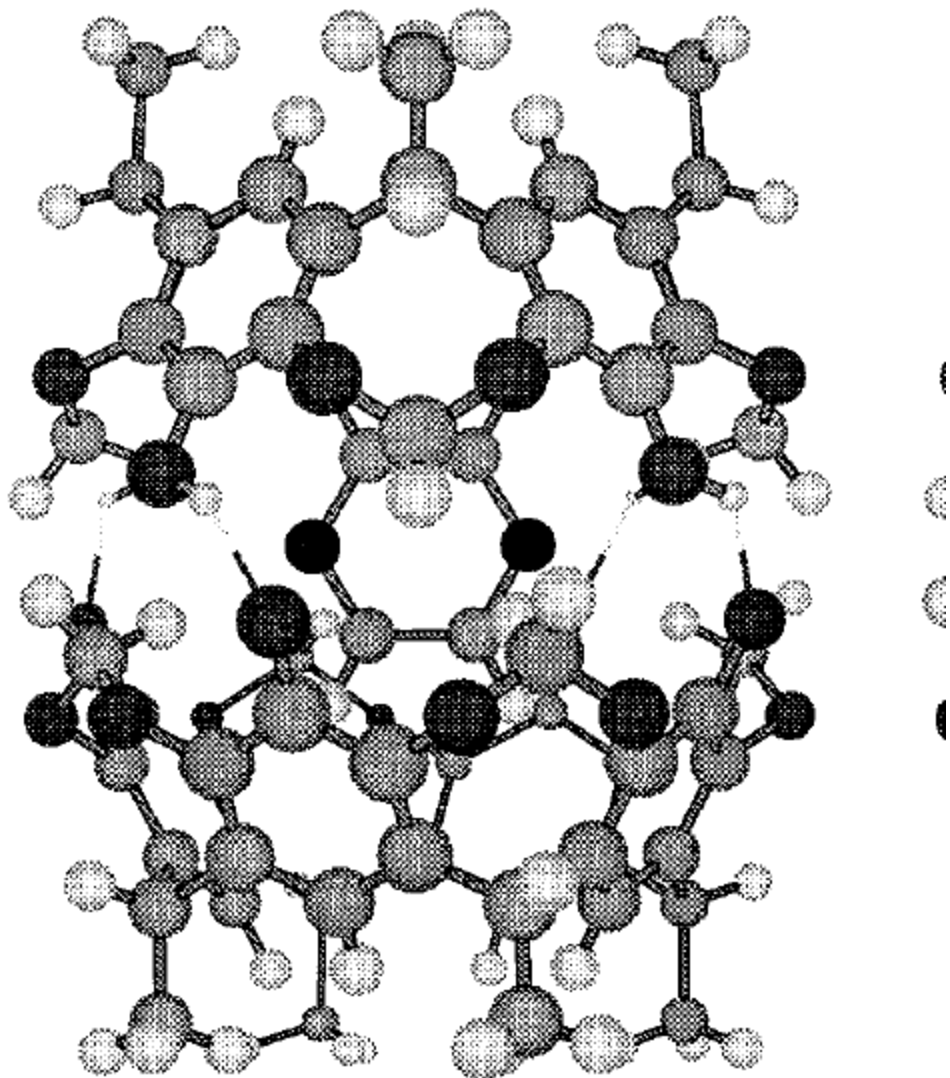






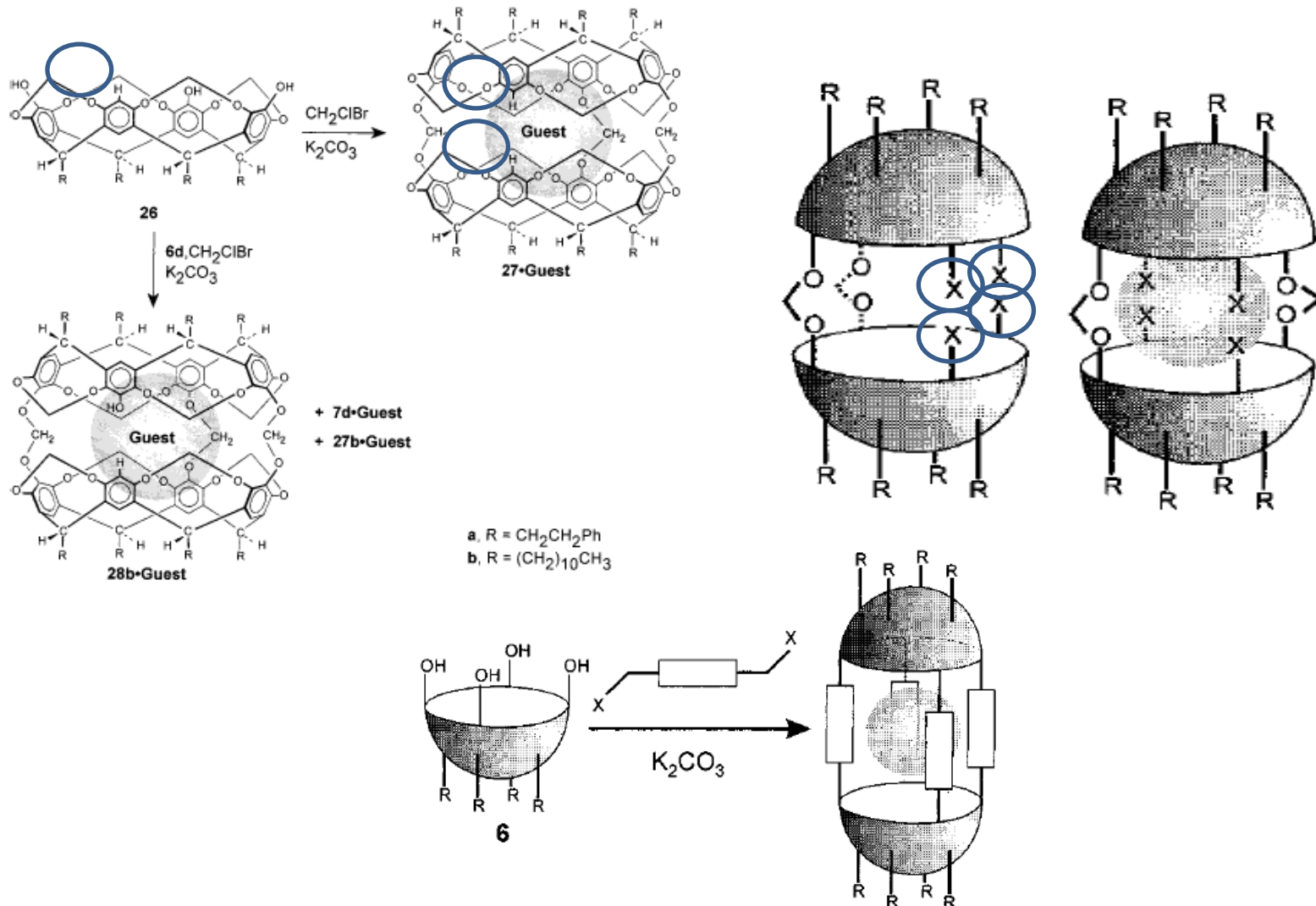
tively. The signals for pyrazine in asymmetric complex **3c**•pyrazine consisted of two *meta*-split doublets at 4.31 ($J = 1$ Hz) and 4.35 ppm ($J = 1$ Hz).¹⁶ This confirms that pyrazine is oriented in complex **3b**•pyrazine with its nitrogens at the equator and its hydrogens extending into the bowls (structure **A**, Figure 3). The activation energy for rotation of pyrazine about the pseudo- C_2 axes in asymmetric complex **3c**•pyrazine was measured by variable-temperature ^1H NMR spectroscopy to be 18 kcal/mol,¹⁷ which agrees well with the 19 kcal/mol activation

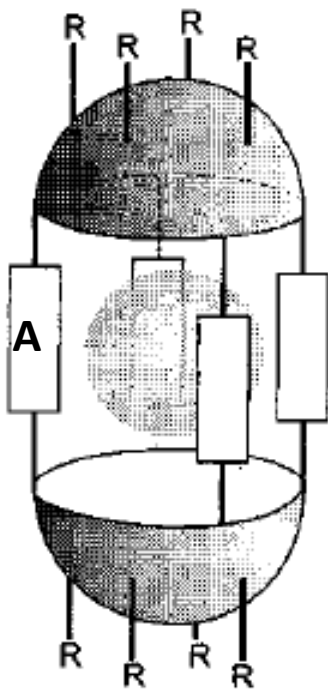
(17) The activation barrier for rotation of pyrazine about the pseudo- C_2 axes of asymmetric complex **3c**•pyrazine was calculated to be 18.3 kcal/mol based on a coalescence temperature (T_c) of 353 K and separation of the signals ($\Delta\delta_{\text{Hz}}$) of 14.3 Hz using the following equation: $\Delta G_c^\ddagger = RT_c - [22.96 + \ln(T_c/\Delta\delta_{\text{Hz}})]$ where ΔG_c^\ddagger is the activation barrier in kcal/mol; T_c is the temperature of coalescence, and $\Delta\delta_{\text{Hz}}$ is the separation of the signals in Hz. See: Abraham, R. J.; Fisher, J.; Loftus, P. *Introduction to NMR Spectroscopy*; Wiley: New York, 1990; pp 194–197.



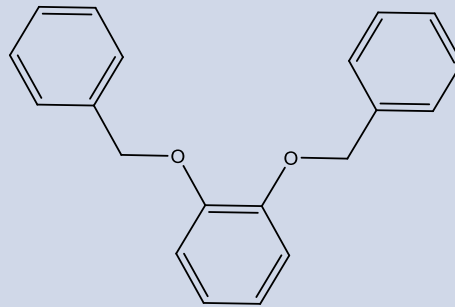
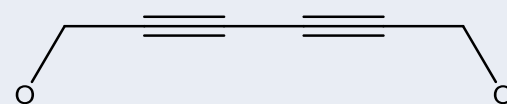
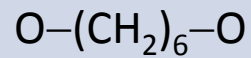
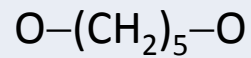
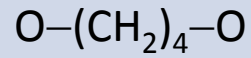
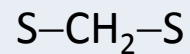
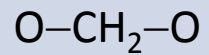
Emicarcerando:

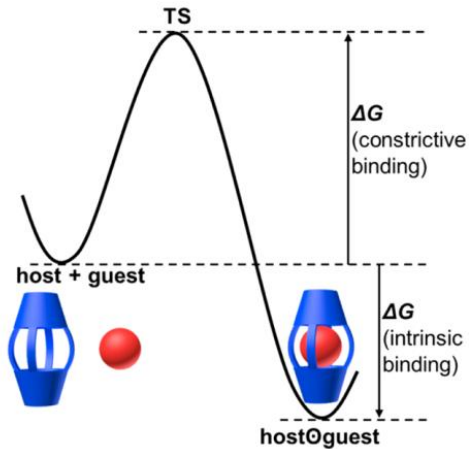
Contenitore molecolare chiuso (capsula) che definisce cavità sferica, i guest sono intrappolati (all'atto della sintesi) - entrata e uscita senza rottura di legame covalente, i.e. velocità di scambio misurabile





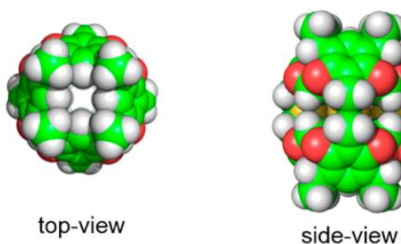
A

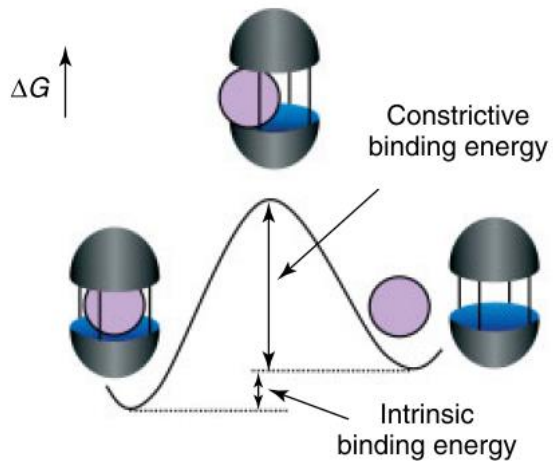




Intrinsic binding, the free energy of complexation, depends on the magnitude of the noncovalent interactions between the guest and the host's inner surface.

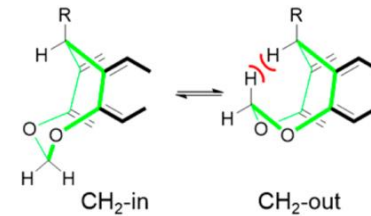
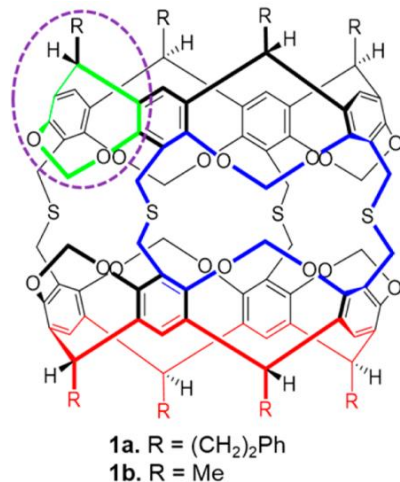
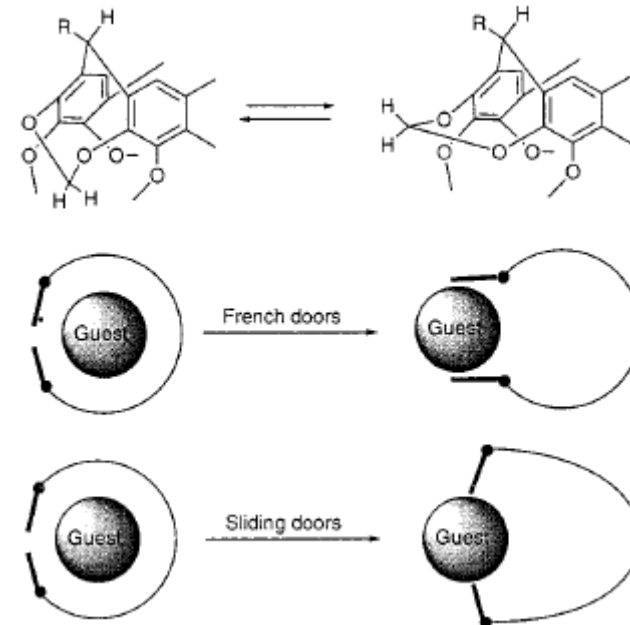
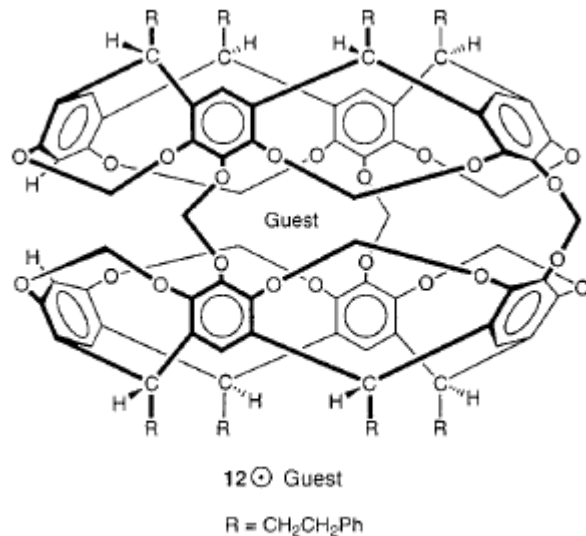
Constrictive binding, activation energy required for a guest to enter the inner cavity of a hemicarcerand through a size restricting portal in the host's skin.





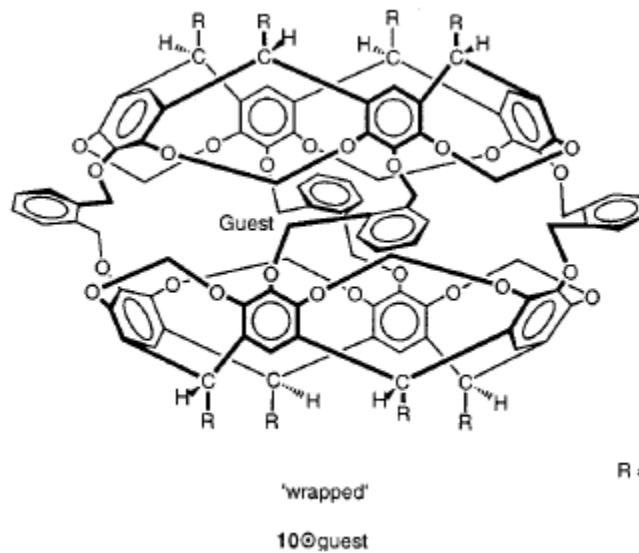
Constrictive binding: aumenta con le dimensioni del guest, diminuisce con le dimensioni dei portali, e con l'aumento della flessibilità dei linker (T).

Gate mechanisms (molecular mechanics calculations) – **French door**
 chair-to-boat transition of the methylene bridges, calculated barrier 22 kcal/mol.

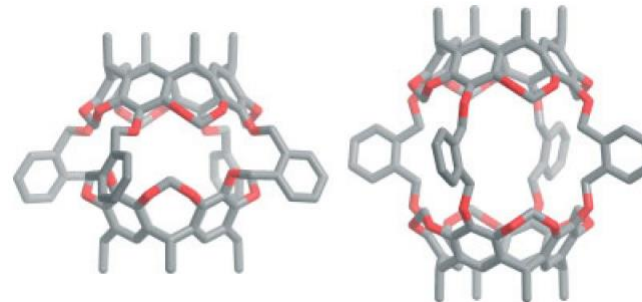
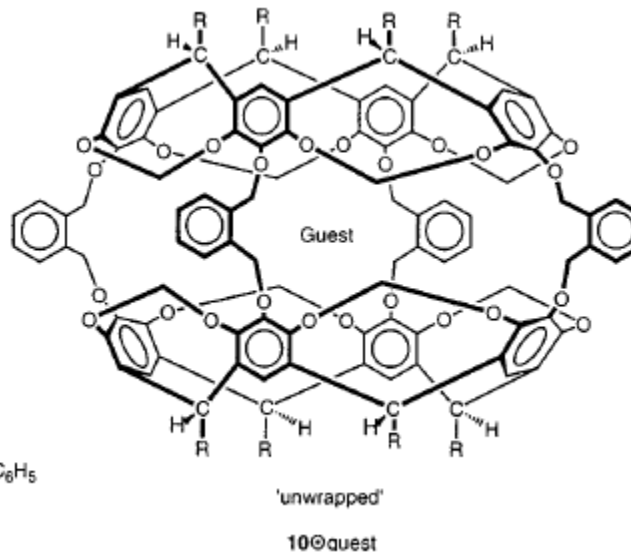


Gate mechanisms (molecular mechanics calculations) – **Sliding door**

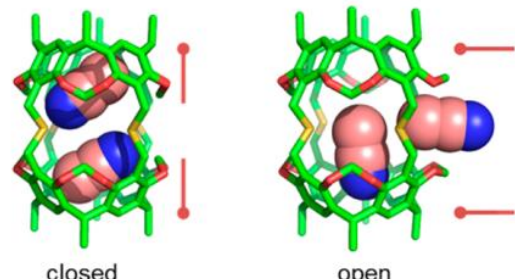
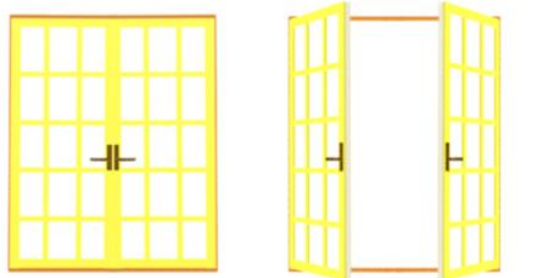
twisting and untwisting of the two host cavitands – measured barrier (VT NMR) 12.6 kcal/mol



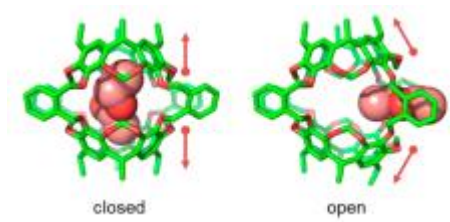
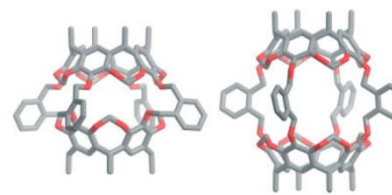
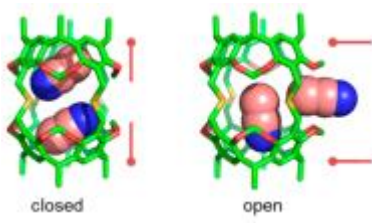
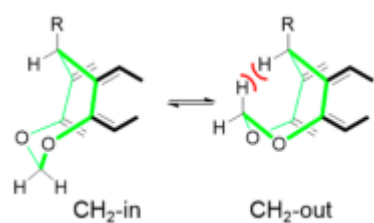
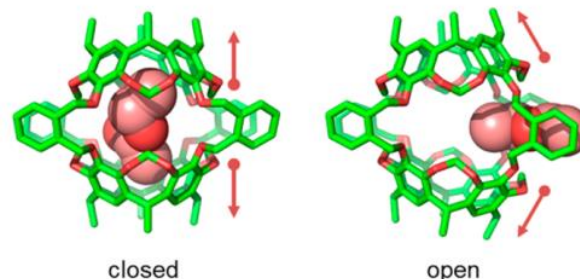
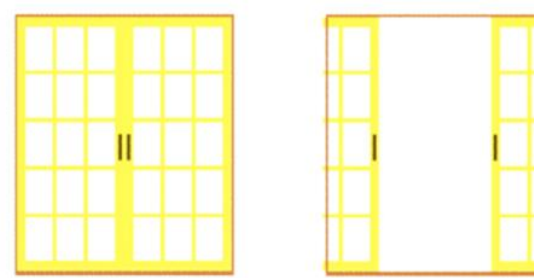
$\text{R} = \text{CH}_2\text{CH}_2\text{C}_6\text{H}_5$

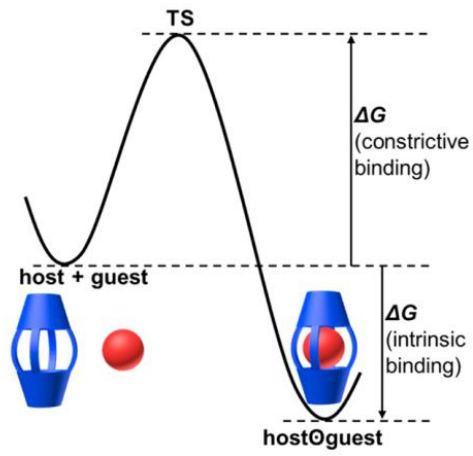


a. French door

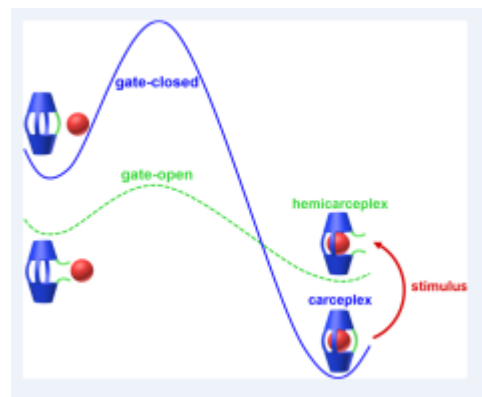
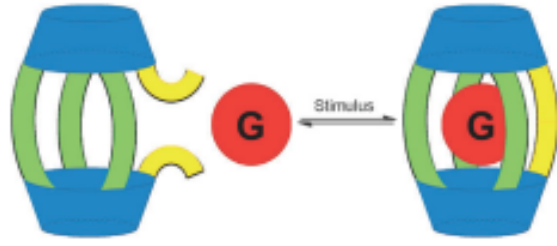


b. Sliding door





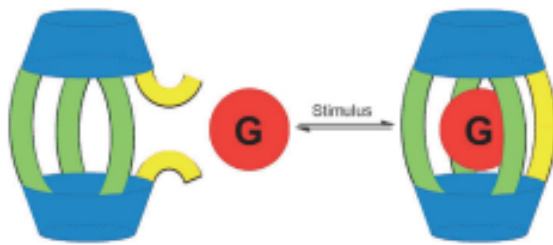
guests. In host–guest systems, there are two energetic quantities associated with guest binding—constrictive and intrinsic binding. The constrictive binding^{11,12} is the activation energy required for a guest to enter the host, while intrinsic binding is the change in energy upon formation of the host–guest complex from free host and guest. Intrinsic binding energy determines the equilibrium constant for binding; the intrinsic binding energy plus the constrictive binding energy determines the kinetic barrier to decomplexation.¹²

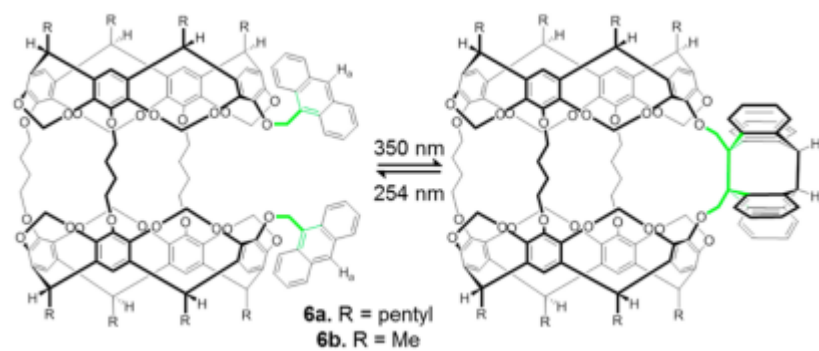
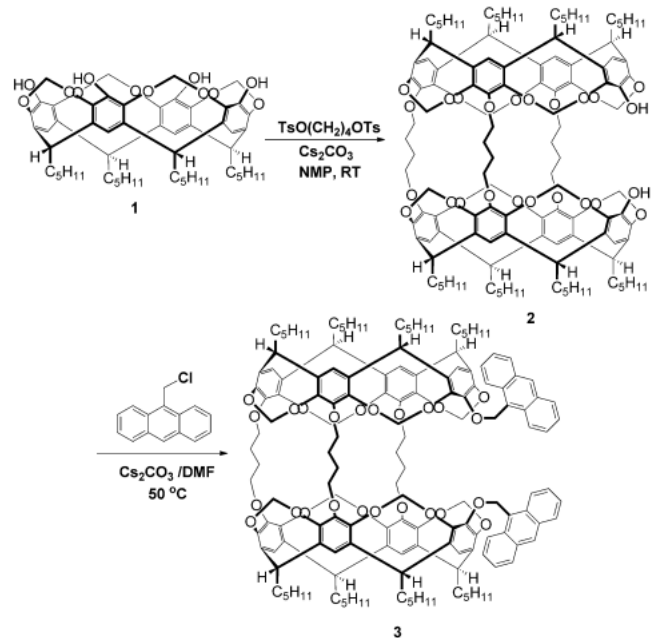


Reversible Photochemically Gated Transformation of a Hemicarcerand to a Carcerand**

Hao Wang, Fang Liu, Roger C. Helgeson, and Kendall N. Houk*

Angew. Chem. Int. Ed. 2013, 52, 655–659





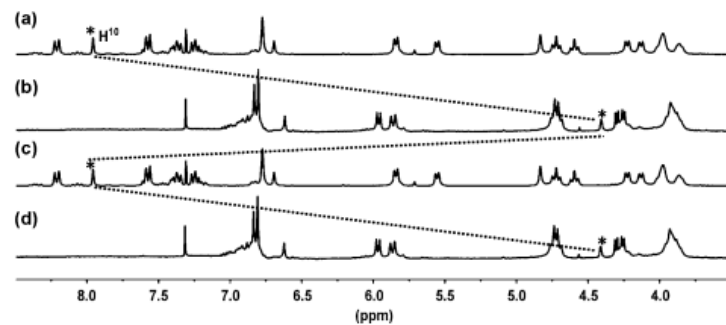
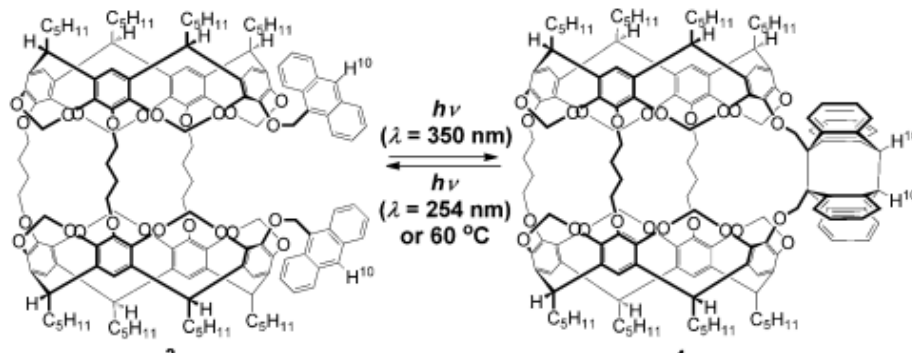
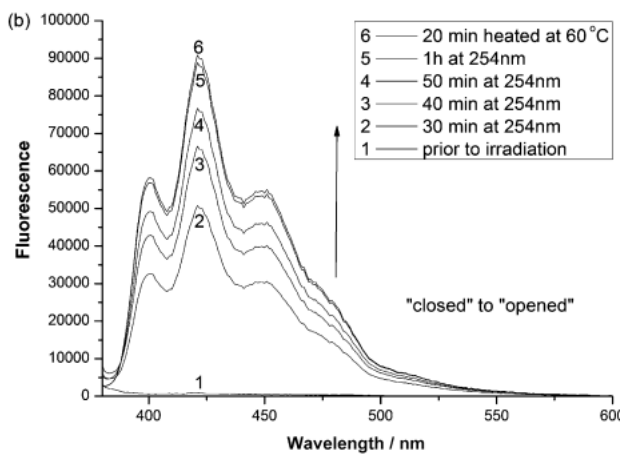
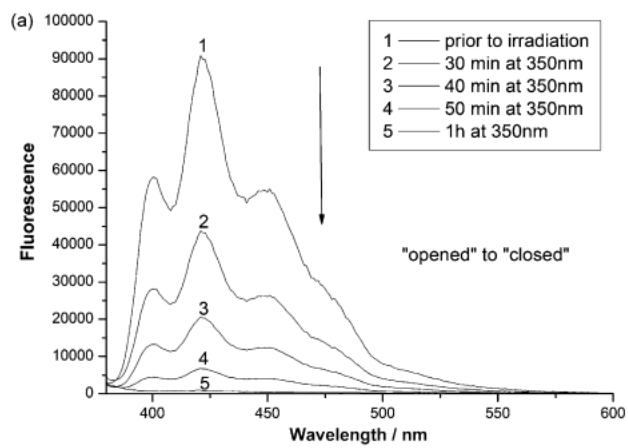
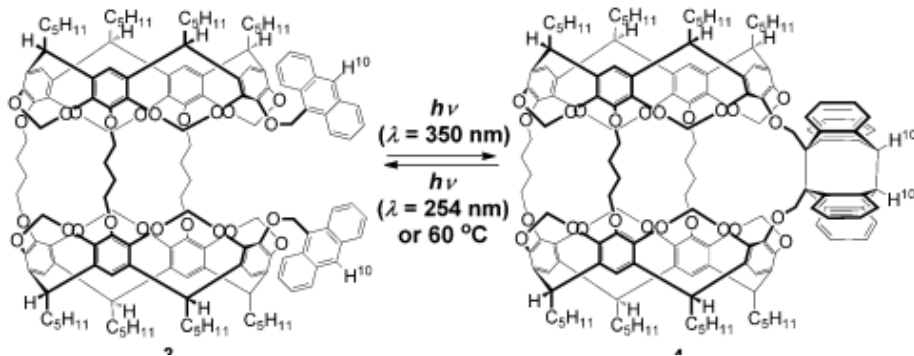
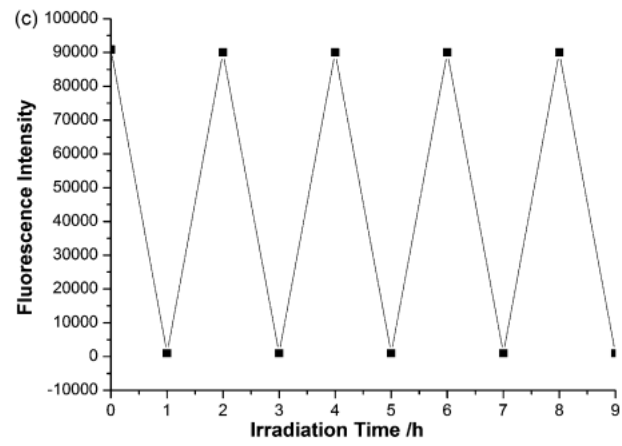
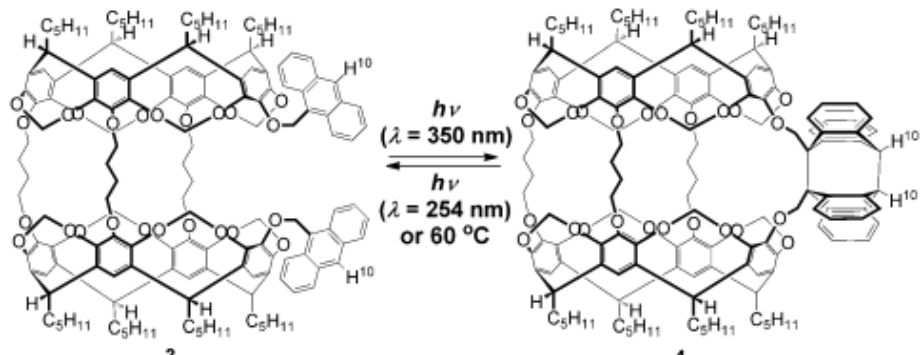
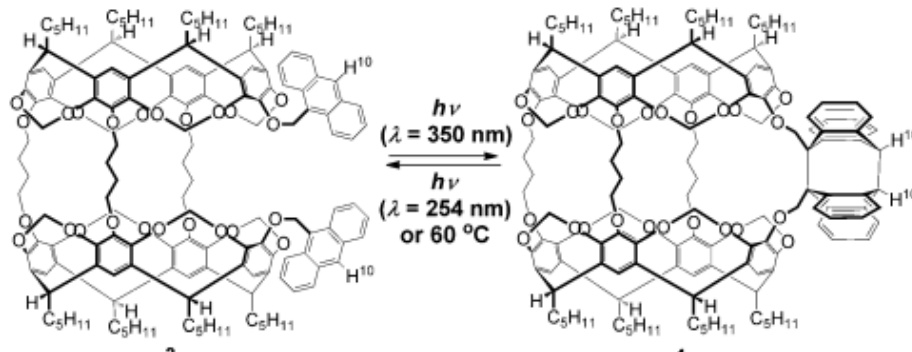


Figure 3. Partial ^1H NMR spectra (400 MHz, CDCl_3) of a) host 3 b) irradiation of host 3 with light at 350 nm for 1 h, c) irradiation of b with light at 254 nm for 1 h or heating at 60°C for 20 min, d) irradiation of c with light at 350 nm for 1 h.







The progress of the photodimerization was also monitored by thin-layer chromatography, which showed only one band after completion of the photodimerization. Photodimer 4 was purified after photolysis at 350 nm. In the high-resolution mass spectrum the molecular ion of photoproduct 4 has the same mass as the parent open-state host 3.

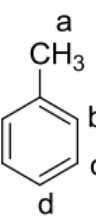
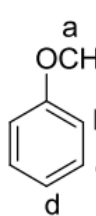
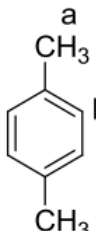
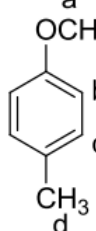
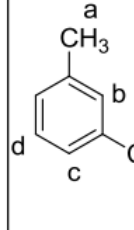
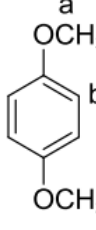
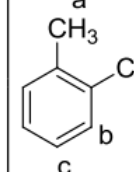
Guest	H	$\Delta\delta$ (ppm)	Guest	H	$\Delta\delta$ (ppm)
	H _a H _b H _c H _d	3.96 1.53 1.85 3.35		H _a H _b H _c H _d	3.87 1.60 1.95 3.30
	H _a H _b	4.17 1.06		H _a H _b H _c H _d	4.01 0.84 0.98 4.21
	H _a H _b H _c H _d	3.17 hidden 1.86 hidden		H _a H _b	4.15 0.85
	H _a H _b H _c	2.34 1.54 1.95	CH _a Cl ₂ —CHCl ₂ CH _a Br ₂ —CHBr ₂	H _a	0.95 1.02

Table S1: Complexation of **4** with various guest molecules and the chemical shift changes of corresponding Hs (before and after complexations) on the guests.

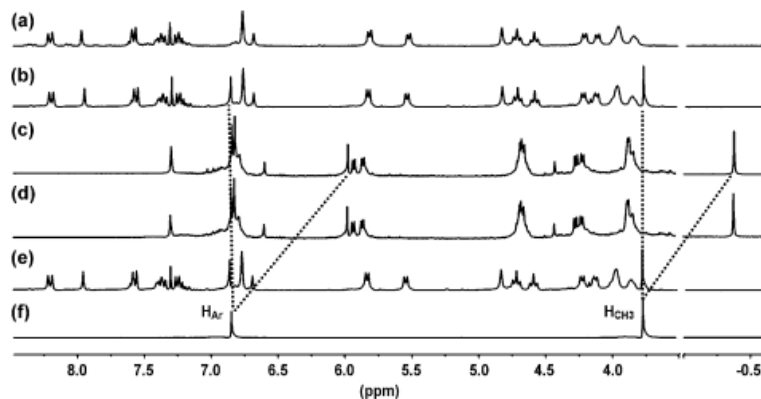
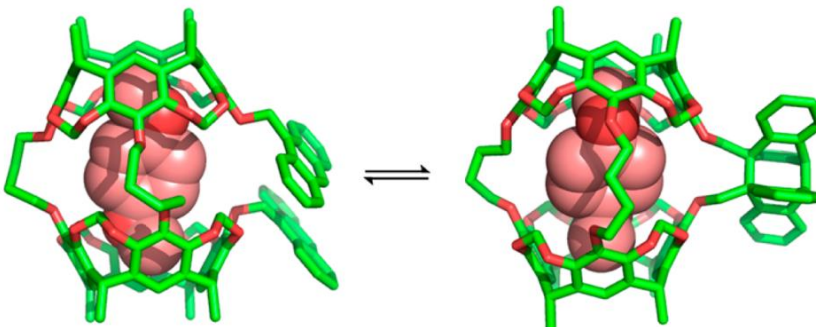
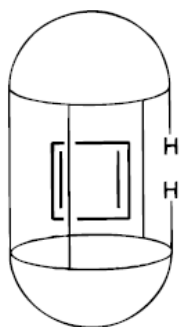
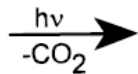
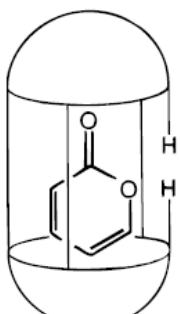


Figure 6. Partial ^1H NMR spectra (400 MHz, CDCl_3) of a) host 3 b) addition of 1 equiv of $1,4-(\text{MeO})_2\text{C}_6\text{H}_4$ into host 3 solution without irradiation, c) $4 \odot 1,4-(\text{MeO})_2\text{C}_6\text{H}_4$,^[16] d) c after 4 weeks in dark and RT, e) irradiation of c with light at 254 nm for 1 h or heating at 60°C for 20 min, f) guest $1,4-(\text{MeO})_2\text{C}_6\text{H}_4$.

The Ph_2O mixture was irradiated at 350 nm for 1 h and then poured into 10 mL of MeOH. The precipitate was dissolved in CDCl_3 and the ^1H NMR spectrum was recorded (F. 6c). The methyl signal of the guest showed a shift from 3.78 to 0.37 ppm ($\Delta\delta = 4.15$ ppm), and the anthracene peaks of 3 disappeared (F. 6c). This indicates that after the gate of 3 is closed, a carceplex is formed between the carcerand 4 and the guest. MALDI mass spectra indicate formation of this carceplex. The carceplex 4@G can stay in the dark at ambient temperature more than 4 weeks without detectable release of the guest molecule (F. 6d). As a result, the activation energy for decomplexation in the open state 3@G and the incarcerated guest can egress easily. The gate-opened hemicarcerand is then almost exclusively filled with the solvent CDCl_3 .

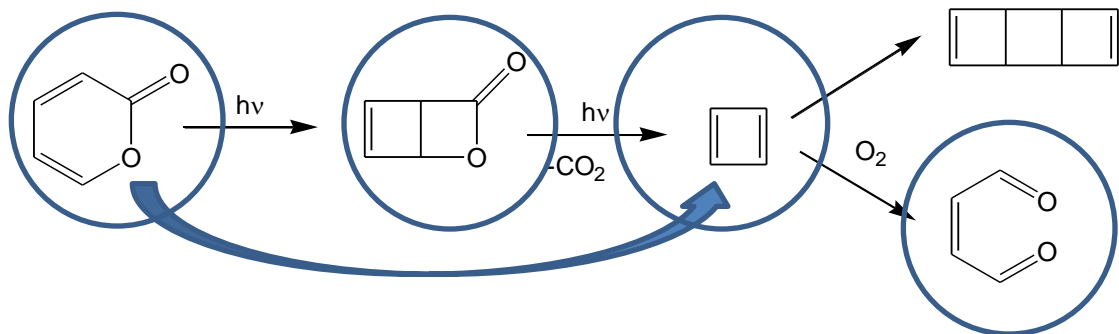


27a•α-pyrone

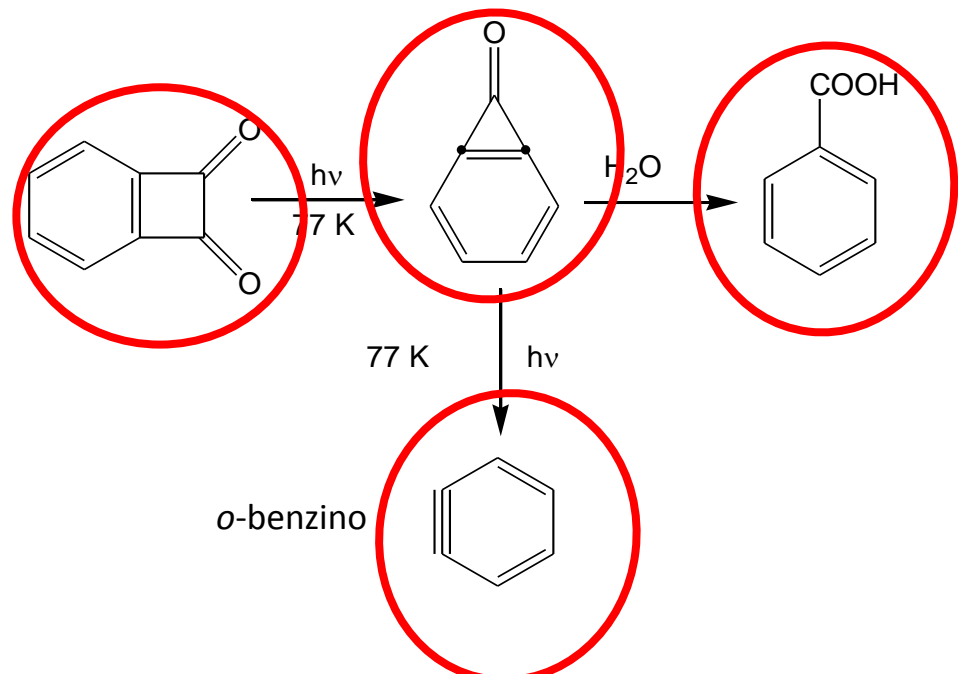
8K - matrice gas inerte congelato

Fotolisi α-pirone a lattame, fotolisi a ciclobutadiene a T amb

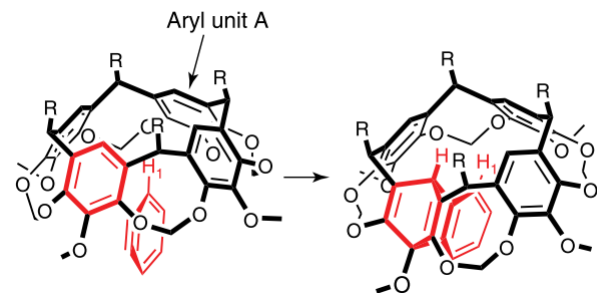
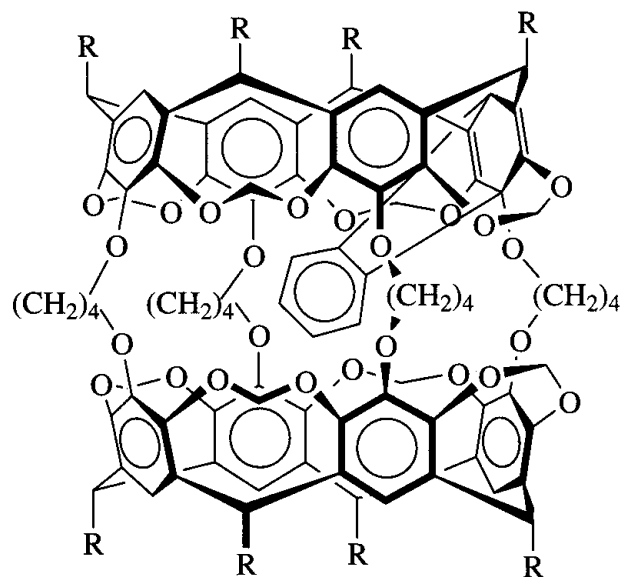
220° (5min), ciclooctatetraene
Aldeide maleica

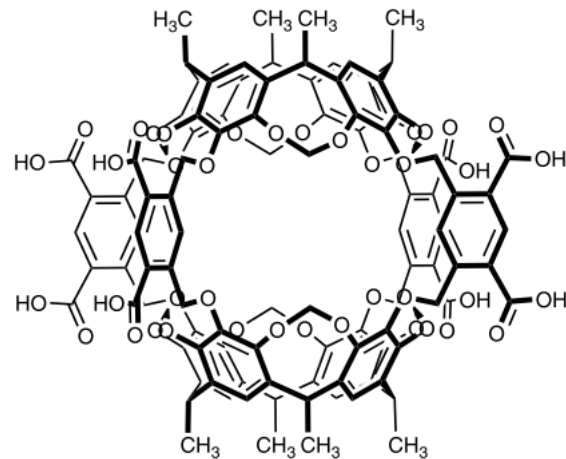


Benzociclobutendione Benzocyclopropenone



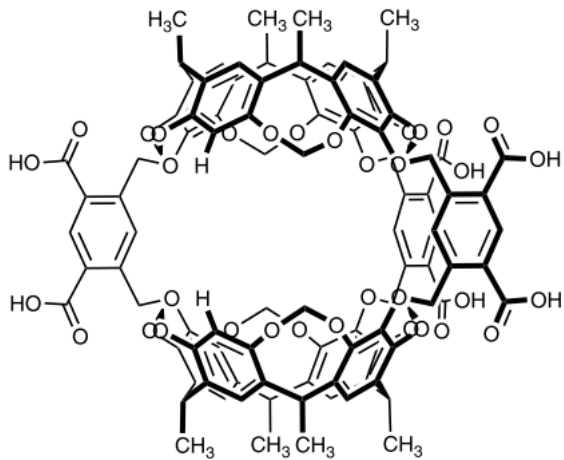
1H e ^{13}C NMR a bassa T



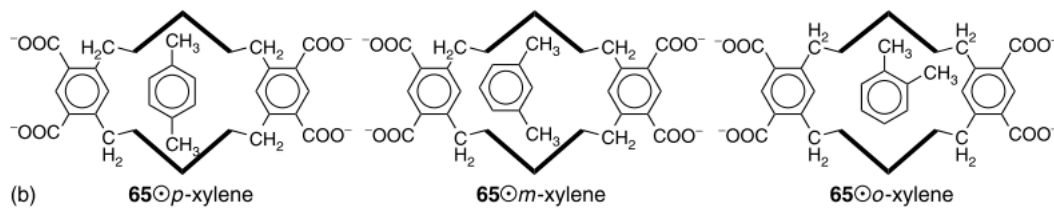


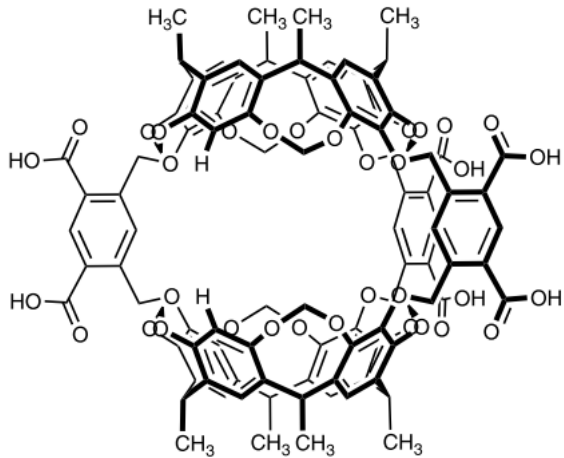
Water soluble octa-acid hemicarcerand:

Hydrophobic effect (higher than cyclodextrines)!

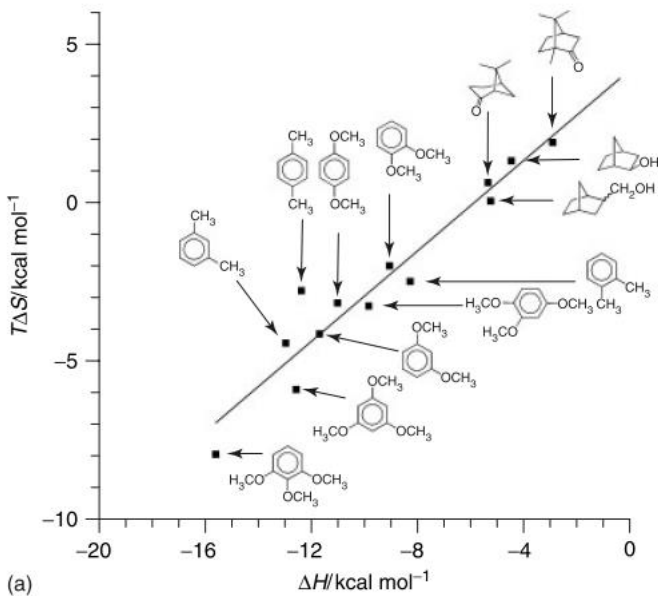


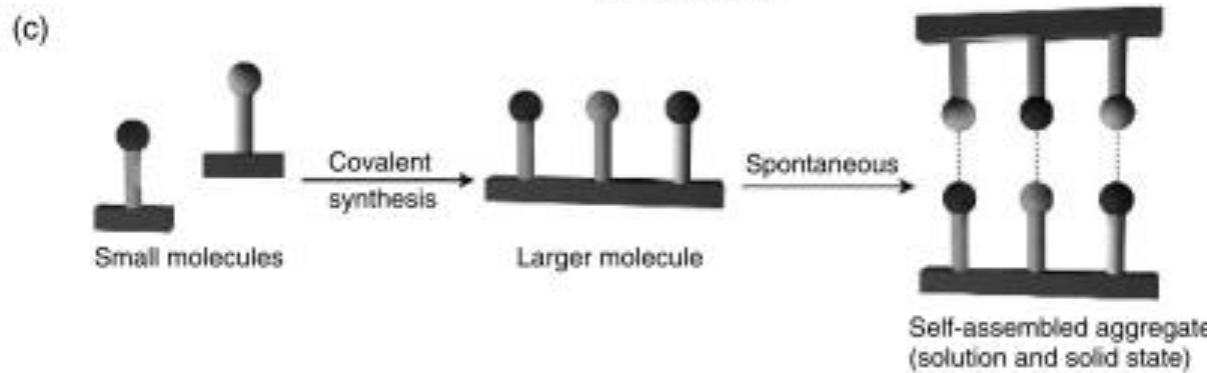
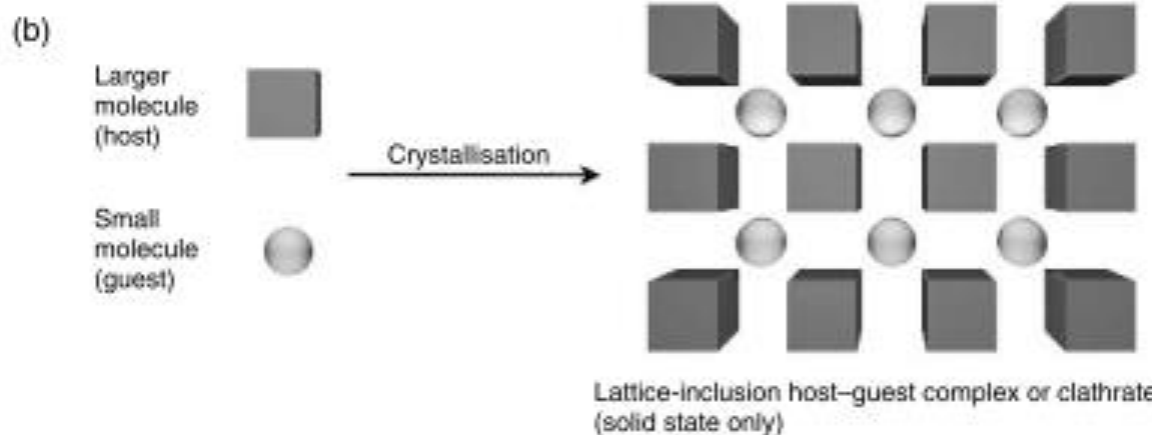
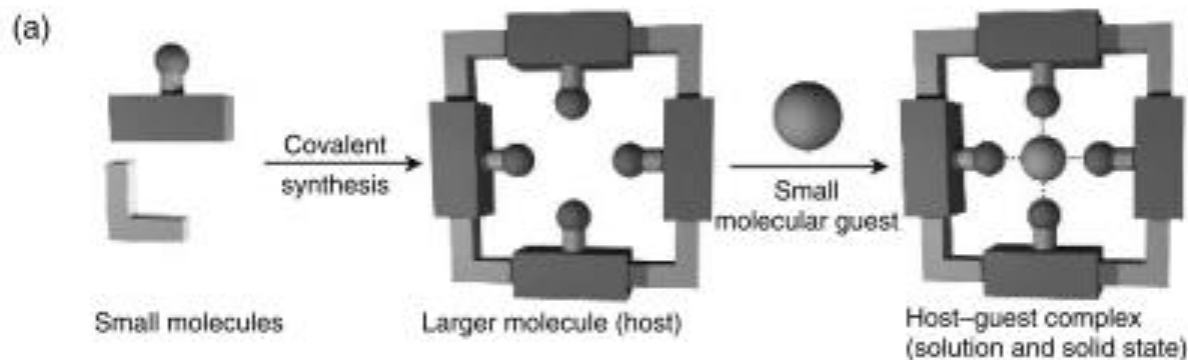
CH- π interactions for isomeric xylenes or dimethoxybenzenes direct the order of affinity:
meta > para >> ortho



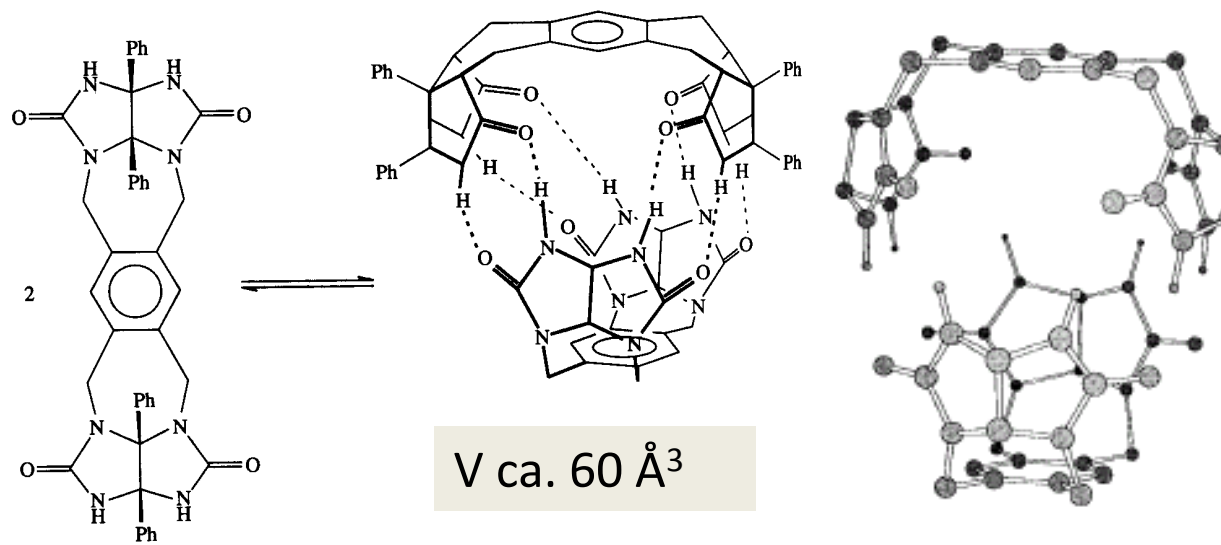
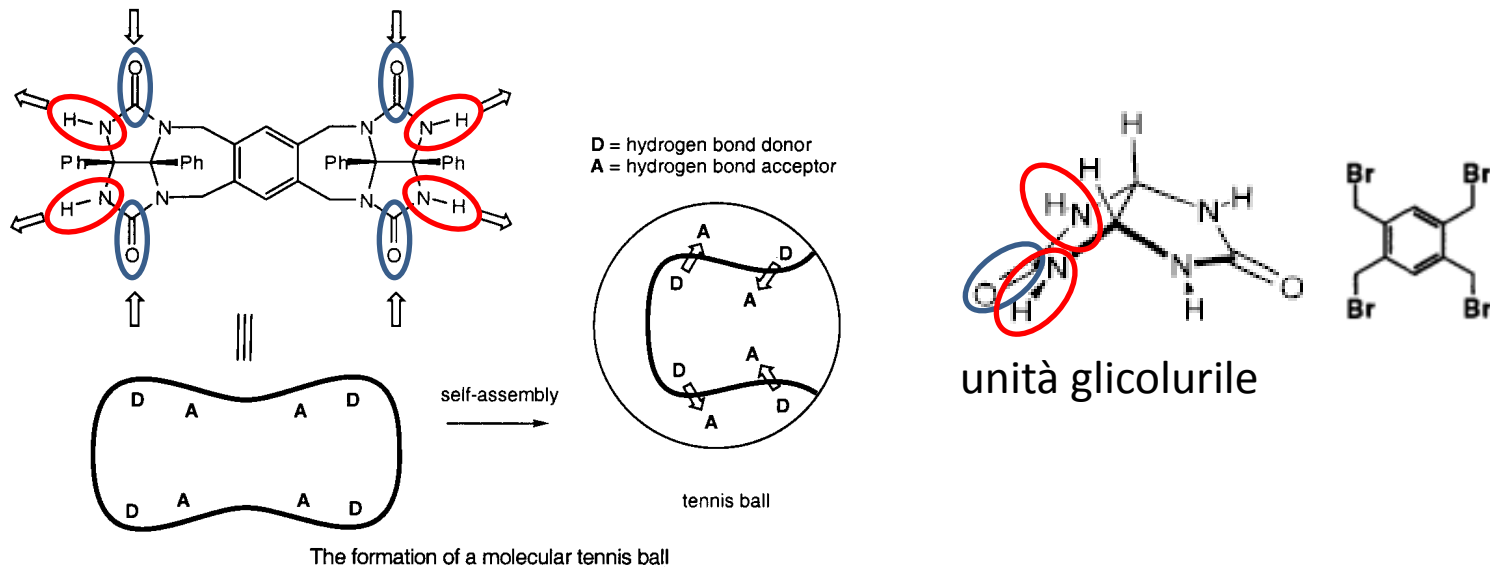


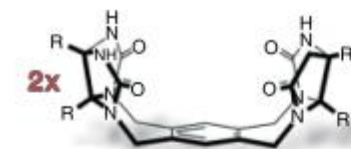
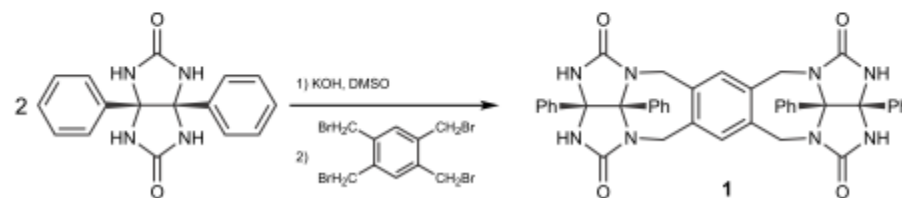
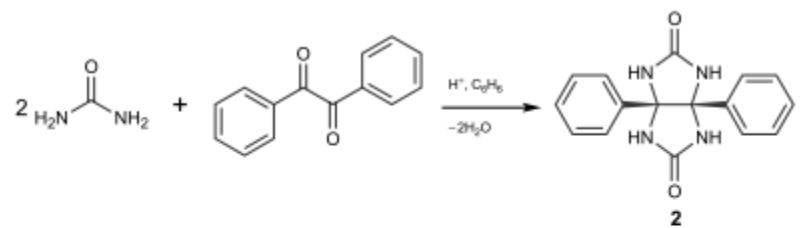
$\text{CH}-\pi$ interactions for isomeric xylenes or dimethoxybenzenes direct the order of affinity:
meta > para >> ortho





Tennis-ball





$\text{R} = \text{C}_6\text{H}_5$

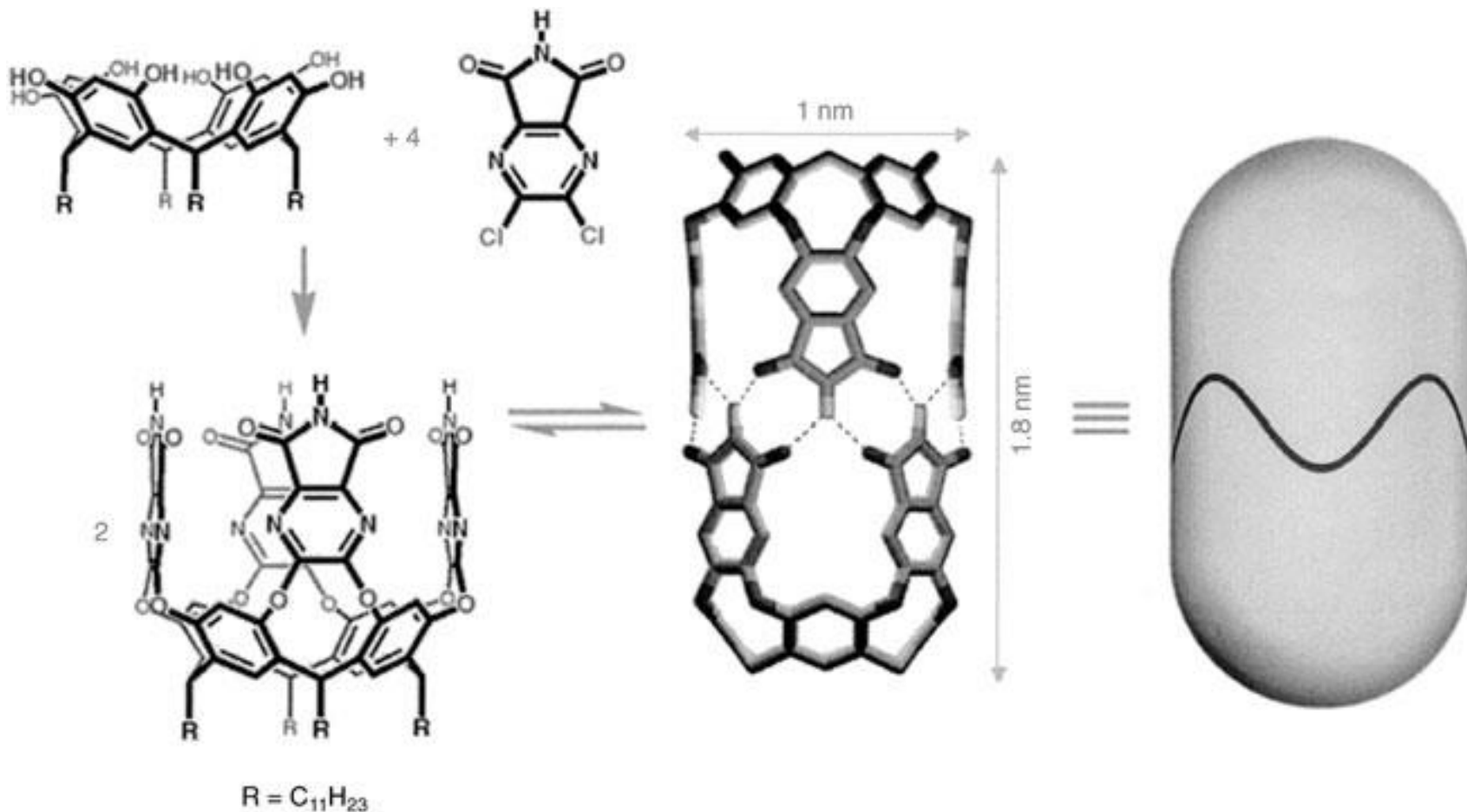


\equiv

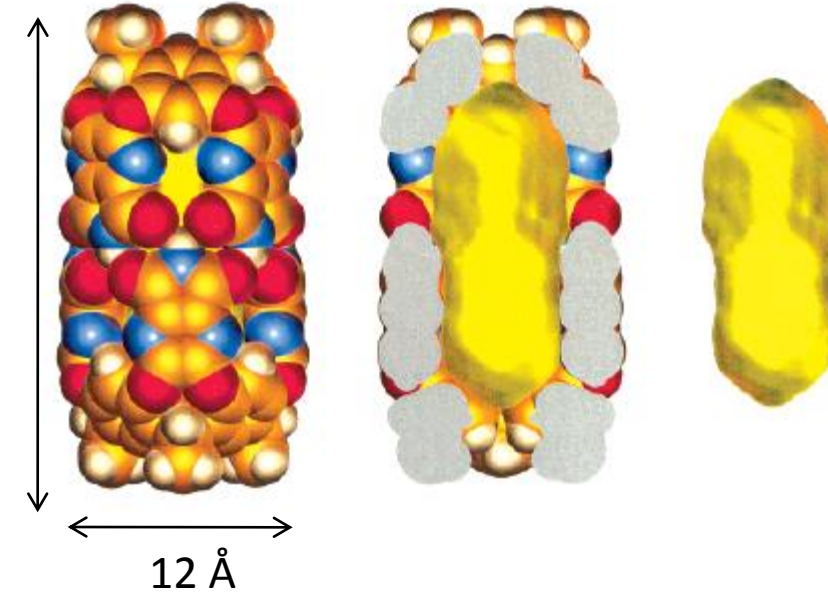
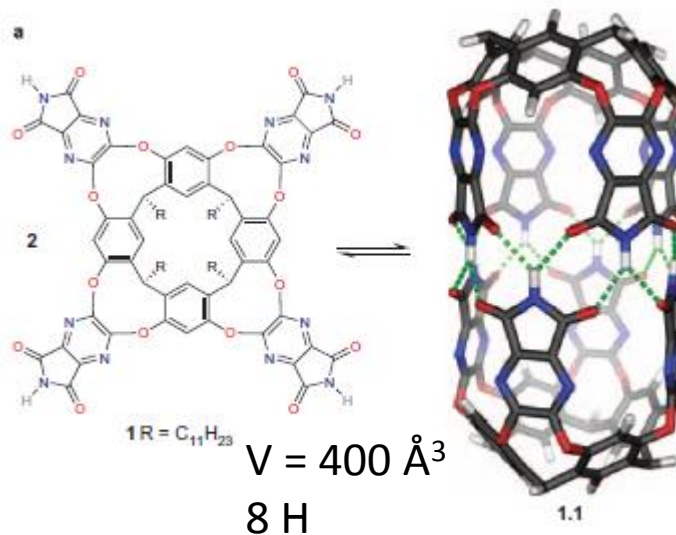
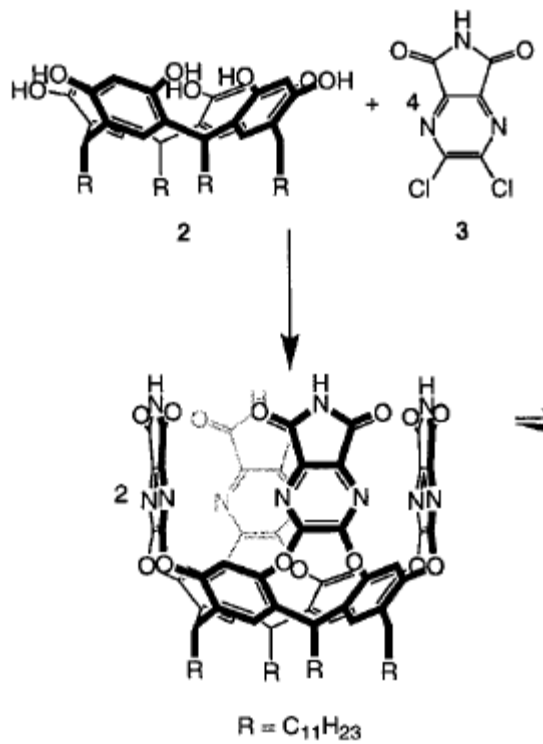


$V \text{ ca. } 60 \text{ \AA}^3$

Molecular Cylinder



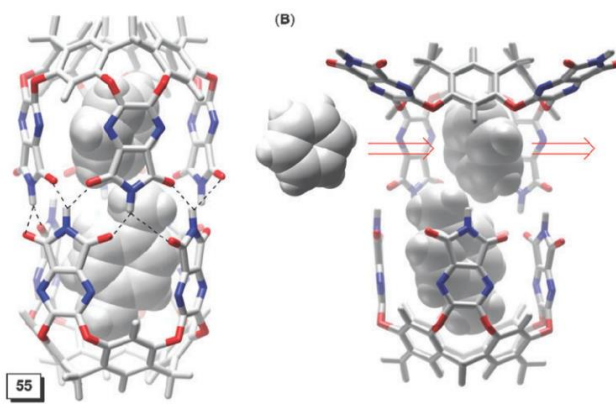
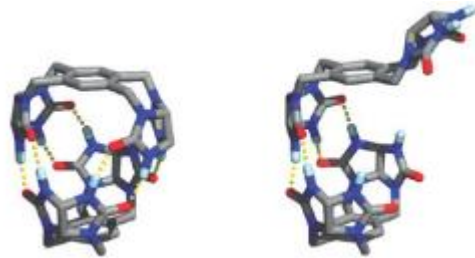
$V \text{ ca. } 420 \text{ \AA}^3$

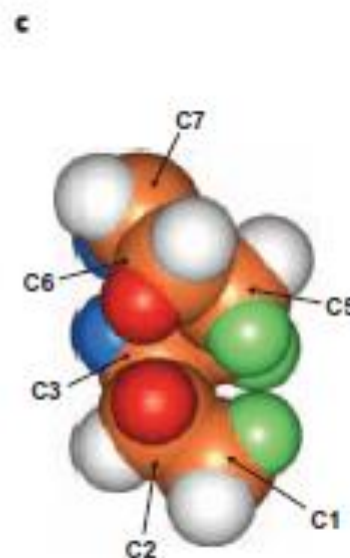
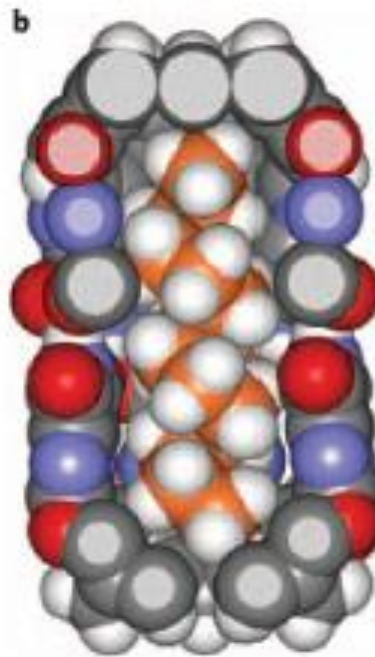


From molecular mechanics calculations:

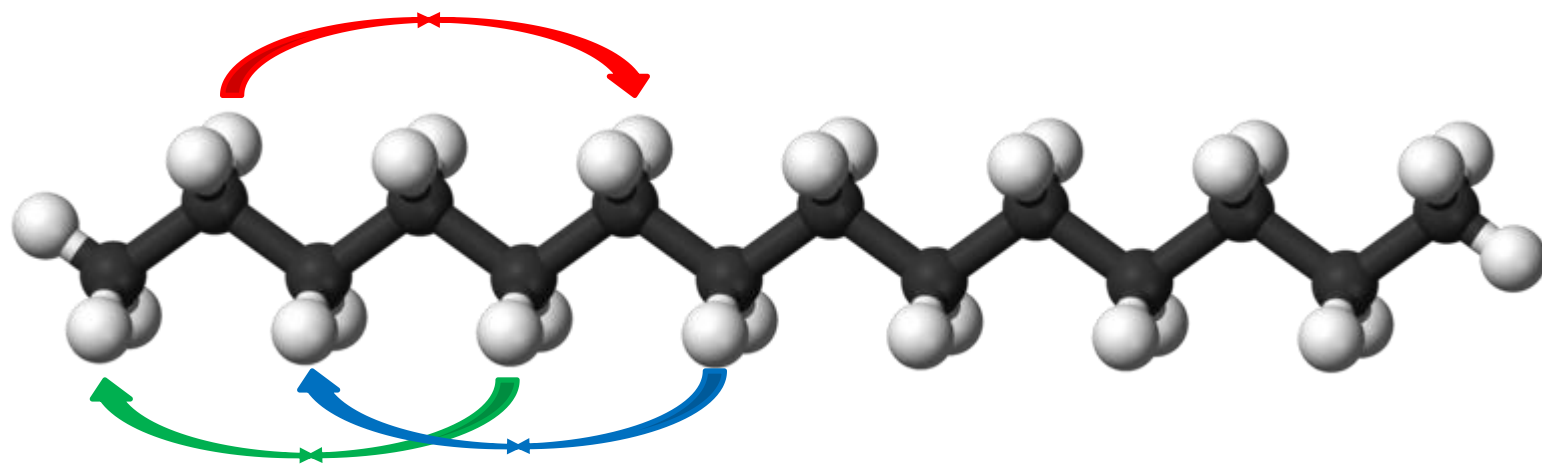
the encapsulated guest(s) occupy approximately 55% of the available space (same occupancy inside most weakly interacting organic solvents).

Stability decreases at higher or lower space occupancy.



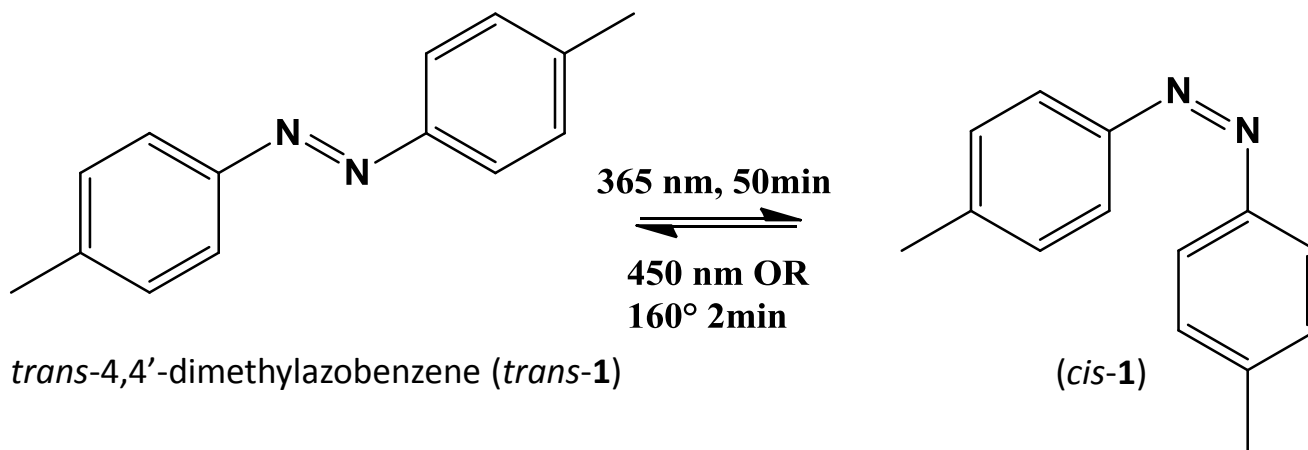


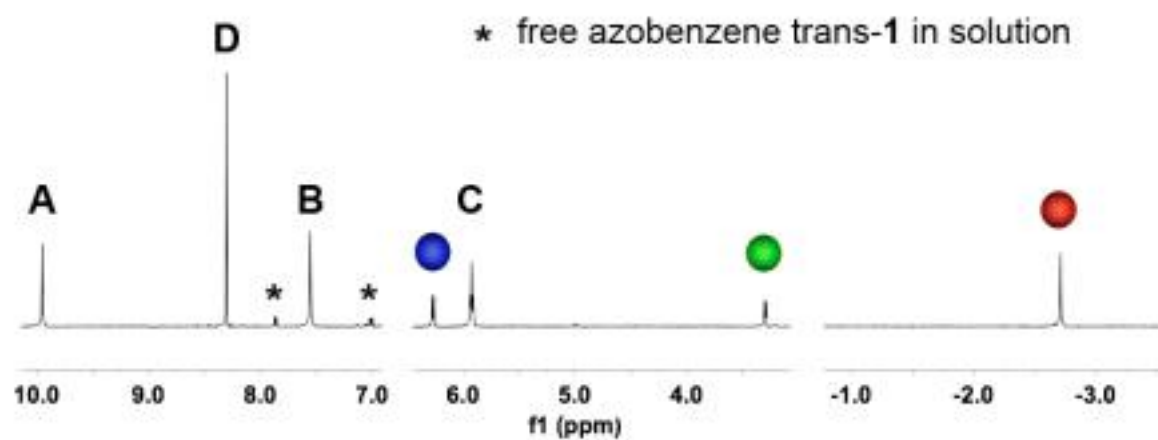
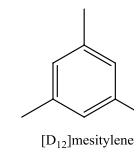
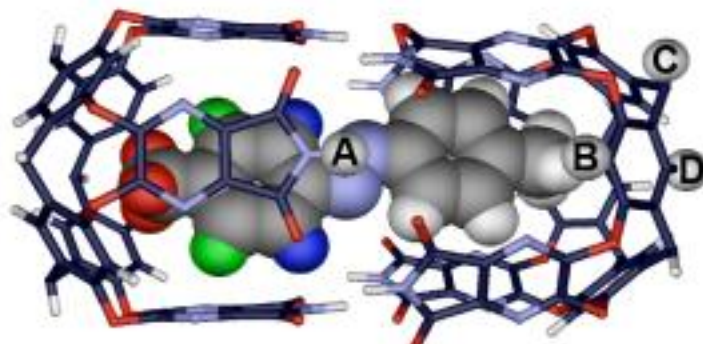
Model structure: encapsulation of coiled alkanes - tetradecane

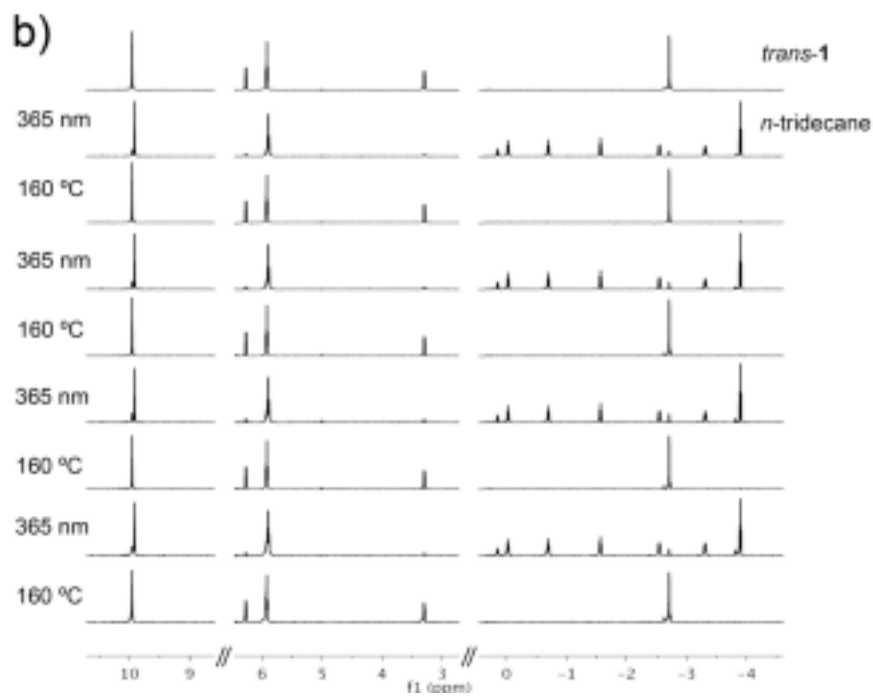
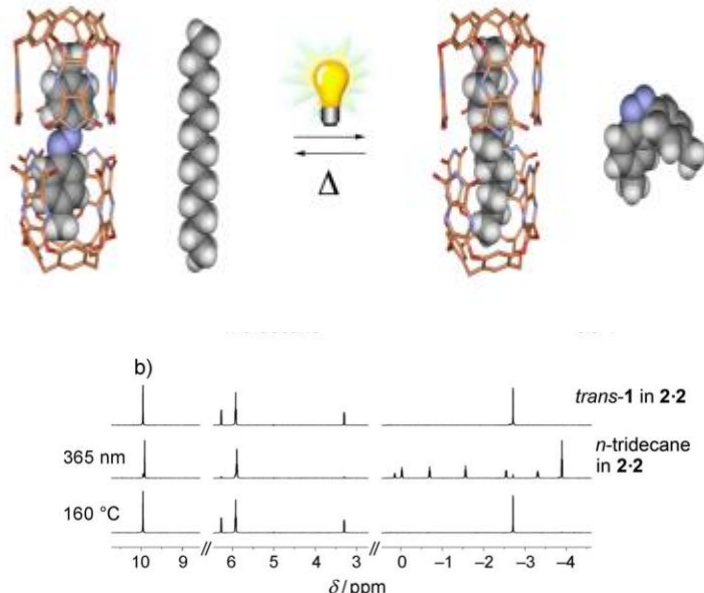
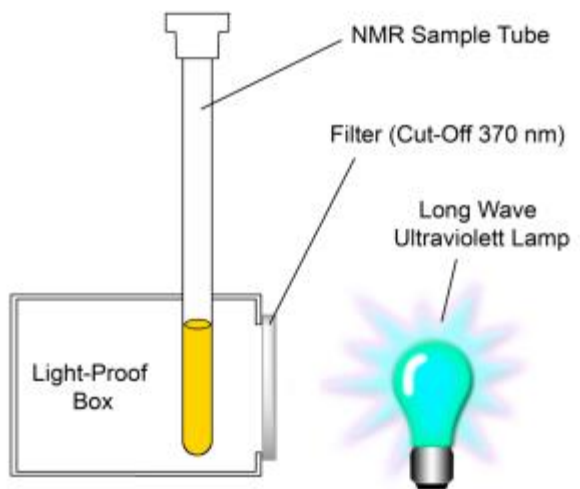


Photochemical Control of Reversible Encapsulation

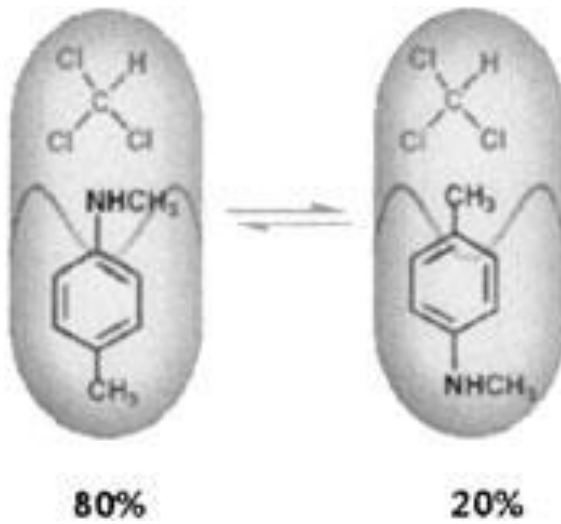
Henry Dube, Dariush Ajami, and Julius Rebek, Jr.*







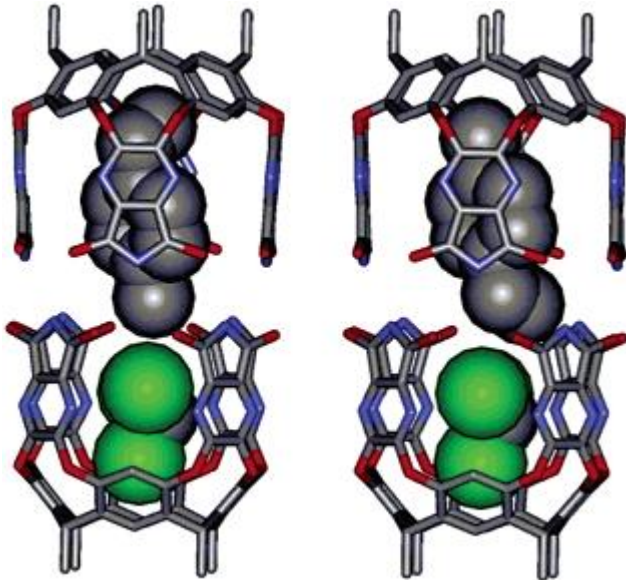
Social Isomers



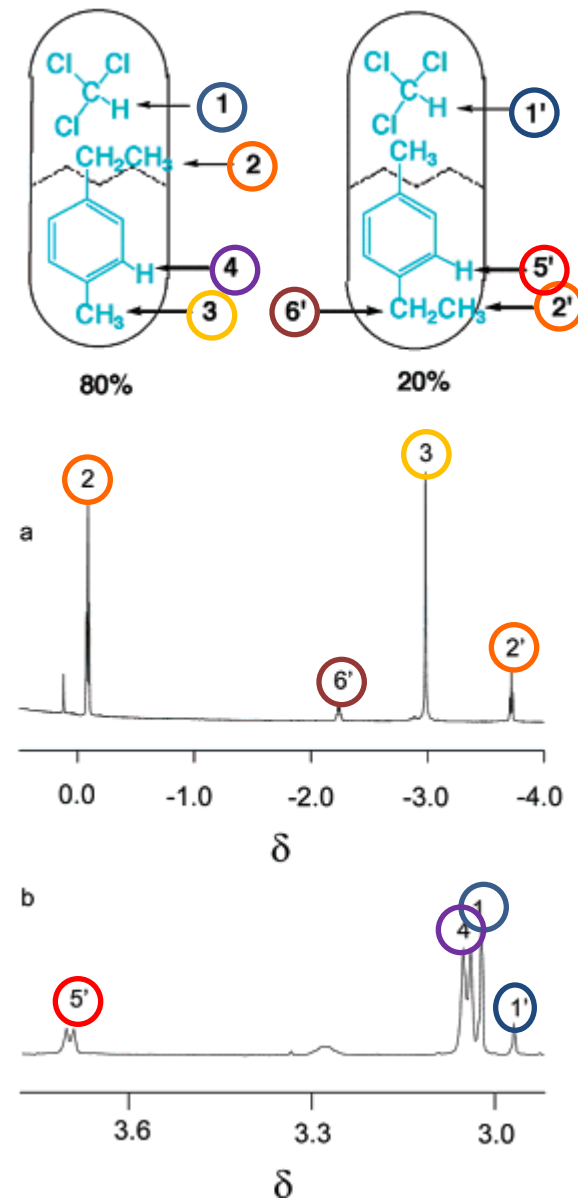
Cloroformio ed N-metil-*para*-toluidina, no interconversione

Social Isomers:

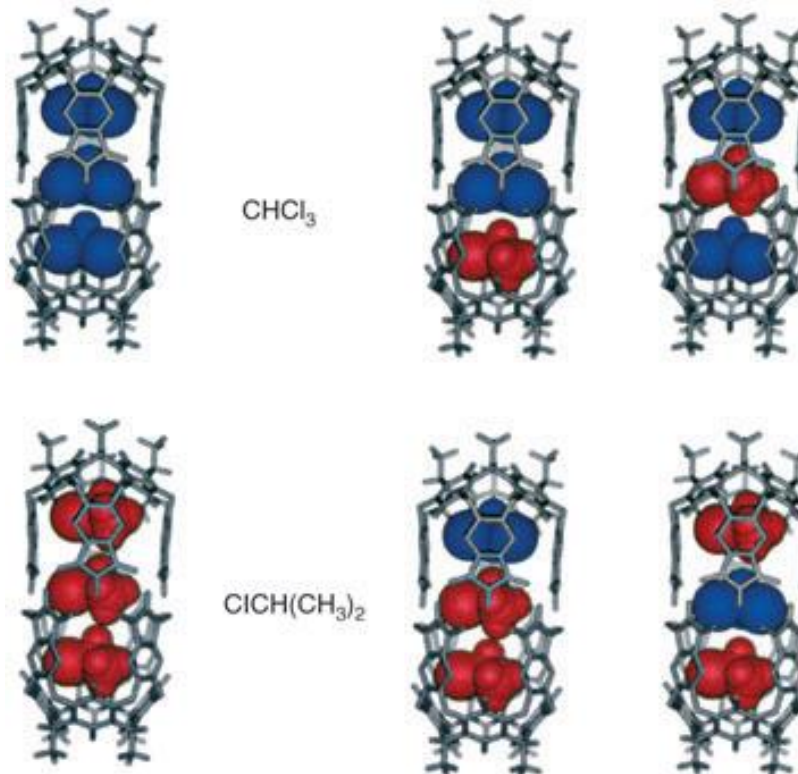
The orientational preference of one guest depends on the presence of the co-guest.



MM optimized structures:
cloroformio e *para*-ethyltoluene



Constellation Isomers



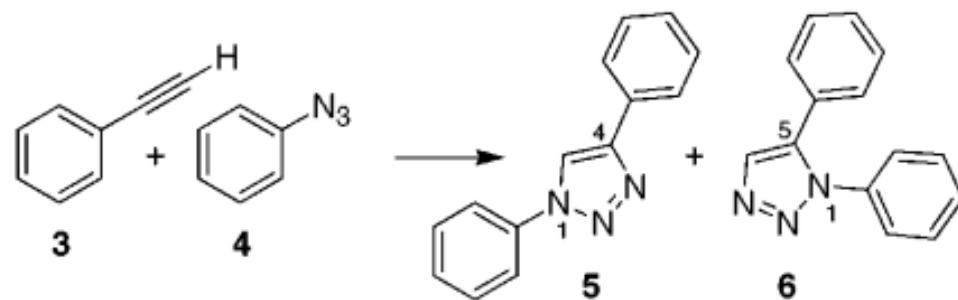
MM optimized structures:
cloroformio e *iso*-propilcloruro

In addition to being able to preserve highly labile species, they may serve as catalysts and accelerate reactions inside their inner cavity by either concentrating the reactants leading to higher effective concentrations or TS stabilization or by preorganising them inside the capsule.

They may create a micro-environment in which two encapsulated reactants are held together in a orientation that differs from their most reactive arrangement in solution (or gas phase) leading to products that are disfavoured in equivalent solution phase reactions.

Reattività nelle capsule molecolari

Cicloaddizione 1,3 regioselettiva di fenilacetilene e fenilazide



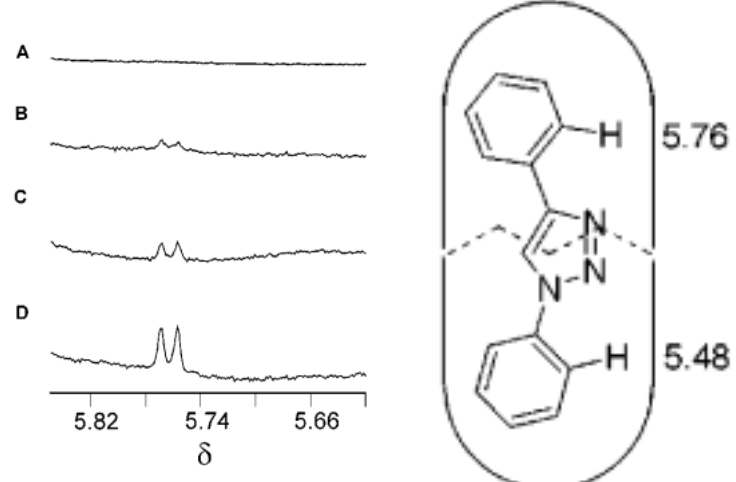


Figure 3. Formation of the 1,4-isomer inside the capsule from phenyl azide (25 mM) and phenylacetylene (50 mM) in the presence of the capsule (5 mM) in mesitylene-*d*₁₂. (A) $t = 0$; (B) $t = 1540$ min; (C) $t = 4320$ min; (D) $t = 8500$ min.

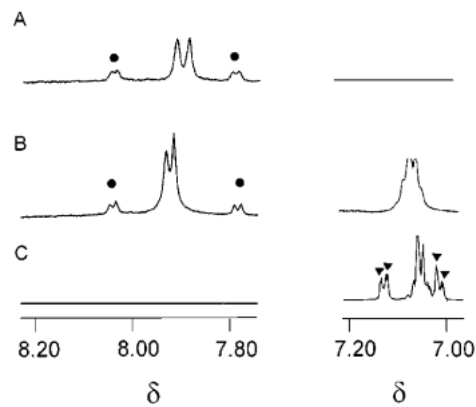
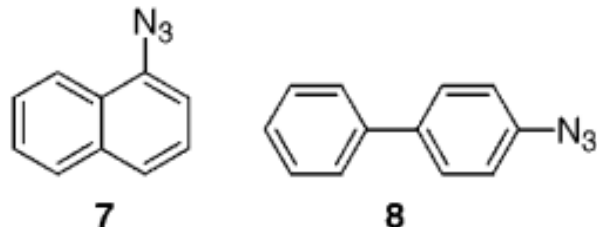
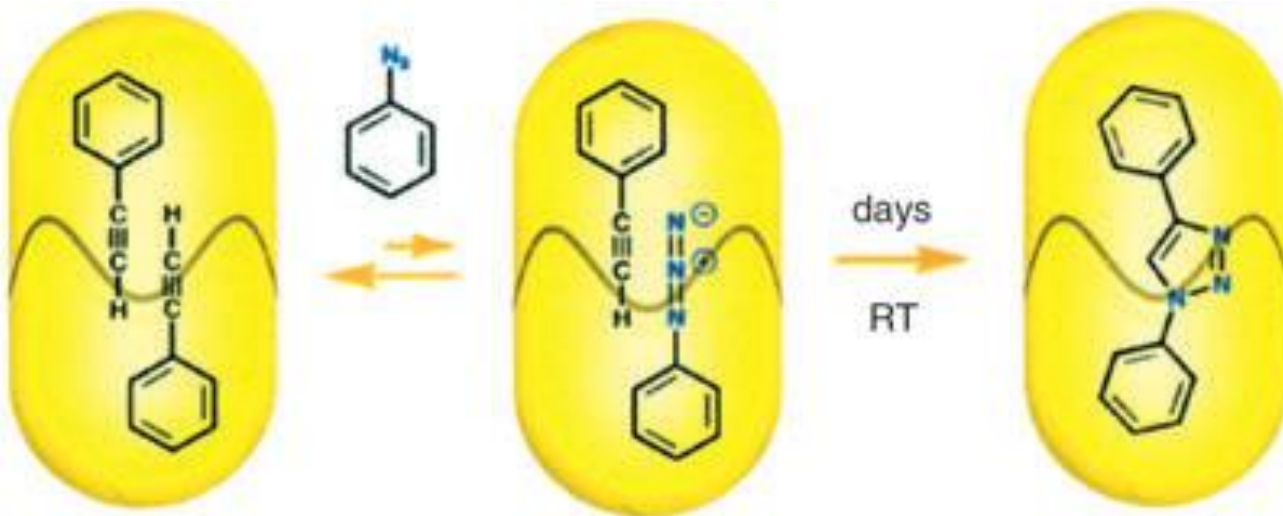


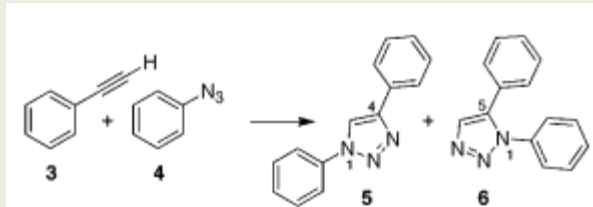
Figure 4. Selective formation of the 1,4-isomer. (A) Addition of DMF-*d*₇ to a solution of authentic encapsulated 1,4-isomer in mesitylene-*d*₁₂. (B) Addition of DMF-*d*₇ to the mesitylene-*d*₁₂ solution obtained from phenyl azide (25 mM) and phenylacetylene (50 mM) in the presence of the capsule (5 mM). (C) Addition of DMF-*d*₇ to solution of authentic 1,5-isomer in mesitylene-*d*₁₂. (●) Released 1,4-isomer; (▽) 1,5 isomer.



Reattività nelle capsule molecolari



Cicloaddizione 1,3 regioselettiva di fenilacetilene e fenilazide:

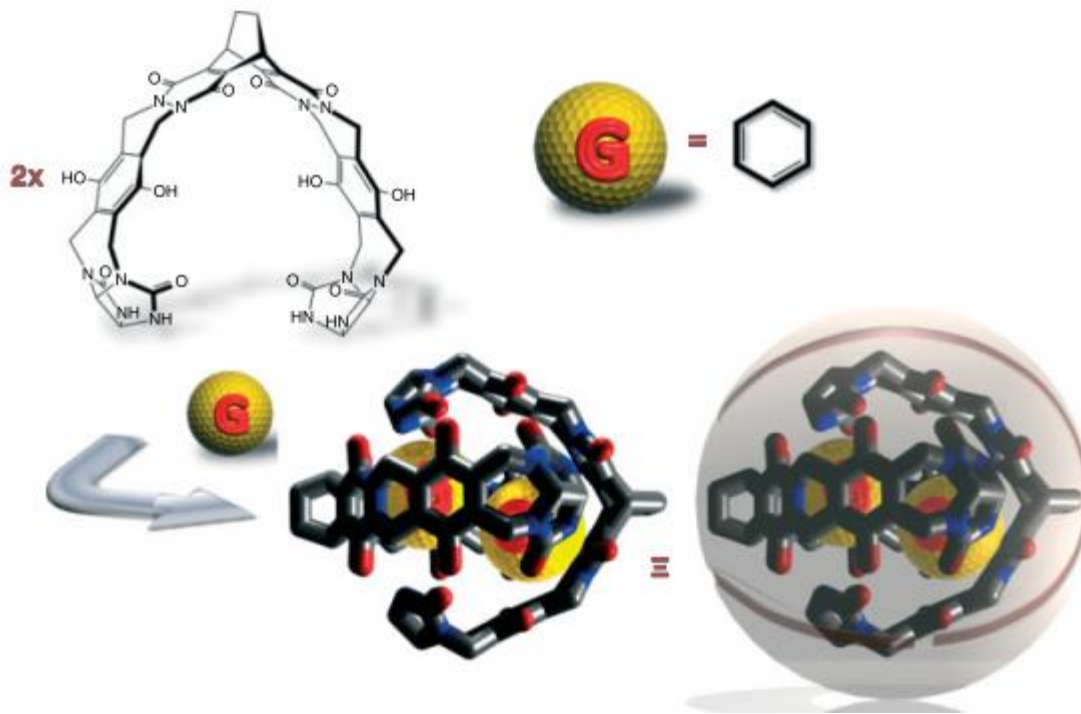


Volume definito = [] 4M vs mM

Tempo di contatto = 1 s vs 1 ns

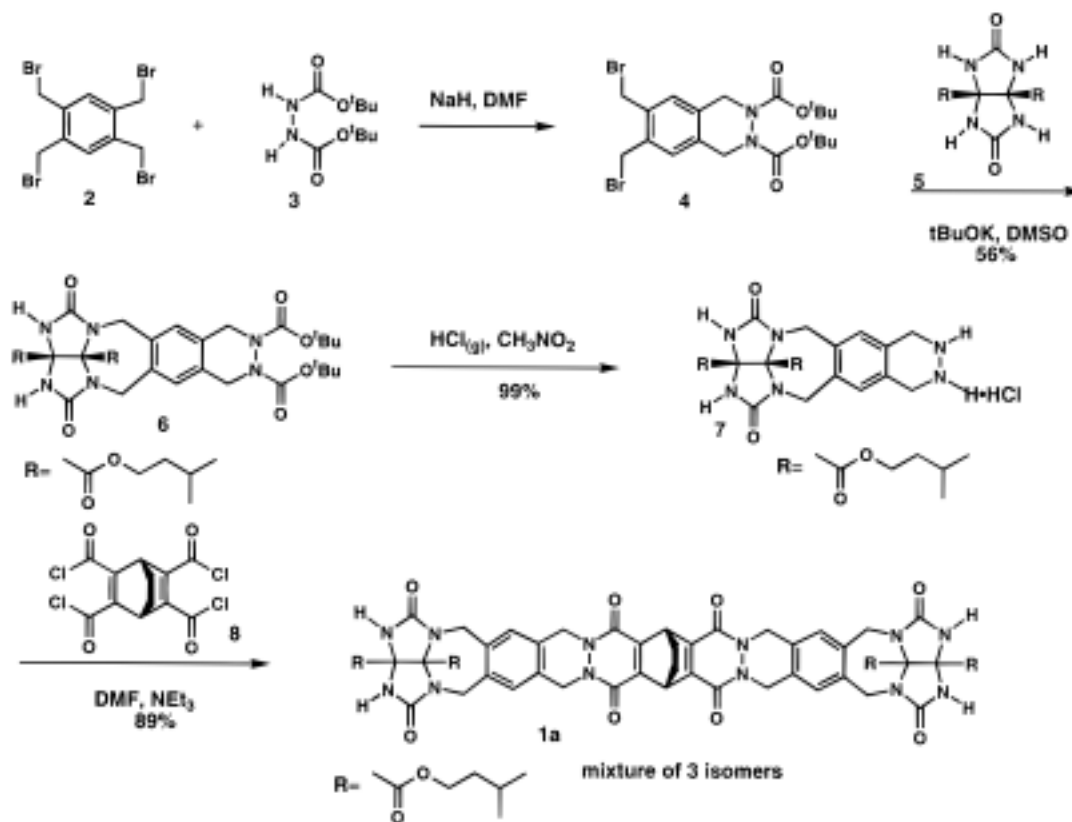
Solvatazione fissa

Soft Ball



V ca. 400 \AA^3

Soft Ball



Reattività nelle capsule molecolari

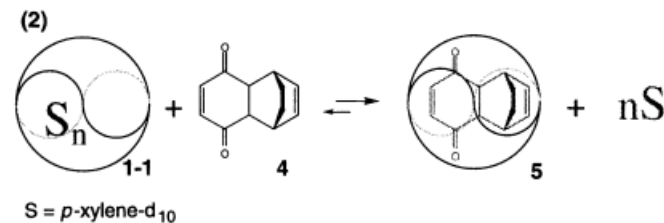
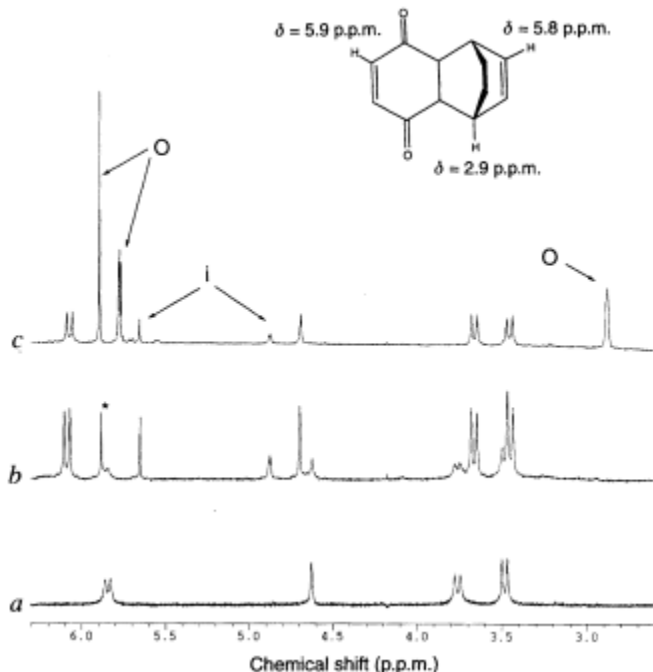
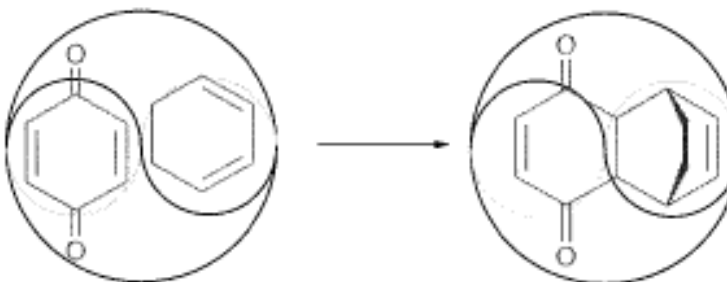
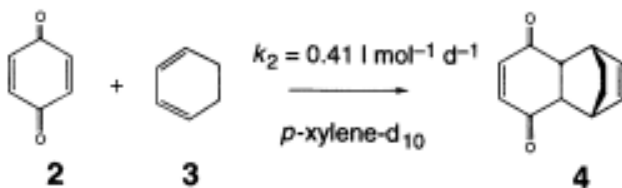


FIG. 2 Proton NMR spectra of **1-1** and its encapsulation complex with the adduct **4** in *p*-xylene-*d*₁₀. Signals of the guest inside the capsule and outside (free) are labelled with 'i' and 'o', respectively. The signal designated with an asterisk represents chloroform. *a*, Compound **1-1** alone. *b*, Compound **1-1** with 0.7 equiv. of Diels–Alder adduct **4** added; all of the latter is encapsulated and separate signals are observed for the complex **5** and solvated dimer **1-1**. *c*, Compound **1-1** with 6 equiv. of Diels–Alder adduct **4** added; all of the capsule is occupied as complex **5** and separate signals are observed for free and encapsulated adduct **4**. Assignments for resonances of free **4** are shown on the structure.

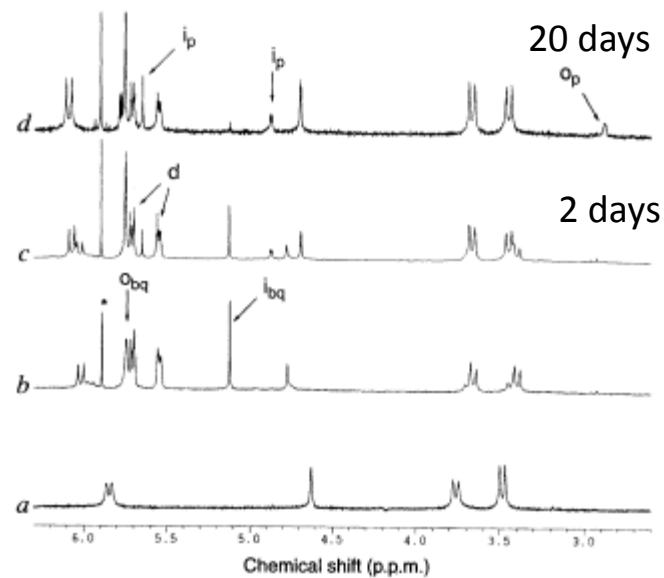
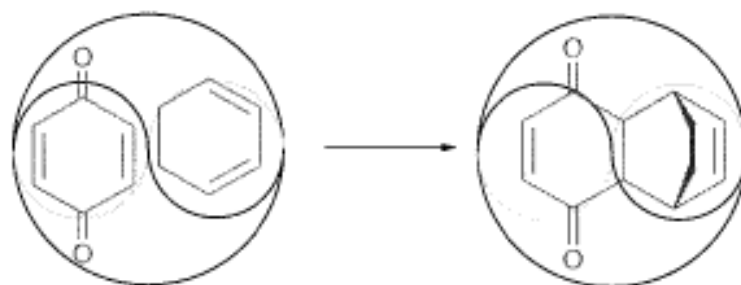


FIG. 3 Changes in the proton NMR spectra of **1-1** during the reaction of *p*-benzoquinone **2** and 1,3-cyclohexadiene **3** in *p*-xylene-d₁₀. The signals for *p*-benzoquinone(bq) and Diels–Alder product (p) inside and outside are designated as 'l' and 'o' respectively. Signals from cyclohexadiene are designated as 'd'. The signal designated with an asterisk represents chloroform impurity. *a*, Compound **1-1** alone. *b*, Shortly after 4 equiv. of *p*-benzoquinone and 4 equiv. of 1,3-cyclohexadiene were added to the solution of **1-1**. *c*, The reaction mixture after 2 days. *d*, The reaction mixture after 19 days, showing evidence of released product and **5** as the principal species.

Reattività nelle capsule molecolari

Cicloaddizione Diels-Alder acceleraz di ca. 200 volte

[] = 5M

Solvatazione

Tempo di contatto



